

# Supernova neutrinos: Earth matter effects and neutrino mass spectrum

C.Lunardini<sup>a)</sup>, A.Yu.Smirnov<sup>b)</sup>

October 30, 2018

*a) SISSA-ISAS, via Beirut 2-4, 34100 Trieste, Italy  
and INFN, sezione di Trieste, via Valerio 2, 34127 Trieste, Italy*

*b) The Abdus Salam ICTP, Strada Costiera 11, 34100 Trieste, Italy  
and Institute for Nuclear Research, RAS, Moscow, Russia*

## Abstract

We perform a detailed study of the Earth matter effects on supernova neutrinos. The dependences of these effects on the properties of the original neutrino fluxes, on the trajectory of the neutrinos inside the Earth and on the oscillation parameters are described. We show that, for a large fraction ( $\sim 60\%$ ) of the possible arrival times of the signal, the neutrino flux crosses a substantial amount of the matter of the Earth at least for one of the existing detectors. For oscillation parameters from the LMA solution of the solar neutrino problem the Earth matter effect consists in an oscillatory modulation of the  $\bar{\nu}_e$  and/or  $\nu_e$  energy spectra. The relative deviation with respect to the undistorted spectra can be as large as  $20 - 30\%$  for  $E \gtrsim 20$  MeV and  $70 - 100\%$  for  $E \gtrsim 40$  MeV. For parameters from the SMA and LOW solutions the effect is localized at low energies ( $E \lesssim 10$  MeV) and is not larger than  $\sim 10\%$ . The Earth matter effects can be revealed (i) by the observation of oscillatory distortions of the energy spectra in a single experiment and (ii) by the comparison between the spectra at different detectors. For a supernova at distance  $D = 10$  Kpc, comparing the results of SuperKamiokande (SK), SNO and LVD experiments one can establish the effect at  $(2 - 3) \sigma$  level, whereas larger statistical significance  $((4 - 5) \sigma)$  is obtained if two experiments of SK-size or larger are available. Studies of the Earth matter effect will select or confirm the solution of the solar neutrino problem, probe the mixing  $U_{e3}$  and identify the hierarchy of the neutrino mass spectrum.

# 1 Introduction

Neutrinos from gravitational collapses of stars stop to oscillate in vacuum long time before they reach the surface of the Earth. For mass squared differences implied by the experimental results on solar and atmospheric neutrinos, the supernova neutrinos arrive at Earth in mass eigenstates. The reason is either the loss of coherence between mass eigenstates on the way from the star to the Earth or the adiabatic conversion from flavour to mass eigenstates inside the star [1].

After a travel of thousands of years, the neutrinos can still be forced to oscillate again: it is enough to put on the way of the neutrinos a filter consisting of flavor non-symmetric matter, like the Moon or the Earth. The neutrinos will oscillate both in the filter and in vacuum after it. Indeed, the eigenstates of the Hamiltonian in matter do not coincide with the mass eigenstates  $\nu_i$ ,  $i = 1, 2, 3$ . So the latter turn out to be mixed and therefore will oscillate:  $\nu_i \leftrightarrow \nu_j$ . As a consequence, oscillations in the flavour content of the flux are realized.

The possibility of oscillations of supernova neutrinos in the matter of the Earth has been discussed long time ago [2]. It was marked that the effect of oscillations can be significant for values of parameters:  $\Delta m^2 \sim 10^{-6} - 6 \cdot 10^{-5} \text{ eV}^2$  and  $\sin^2 2\theta > 2 \cdot 10^{-2}$ . The effect is different for detectors with different trajectories of the neutrinos inside the Earth, and studying the oscillation effects in these detectors one can restore the direction to the supernova [2].

The detection of the neutrino burst from SN1987A triggered a number of new studies of oscillations of supernova neutrinos and, among them, of oscillations inside the Earth. It was suggested that the difference in the Kamiokande-2 (K2) and IMB spectra of events could be related to oscillations of  $\bar{\nu}_e$  in the matter of the Earth and to the different positions of the detectors at the time of arrival of the burst [3]. For this mechanism to work one needs  $\Delta m^2 \sim 10^{-5} \text{ eV}^2$  and large mixing of the electron neutrinos.

The first two K2 events showed some directionality with respect to the supernova. The interpretation of these events as due to the scattering of electron neutrinos from the neutronization peak on electrons put strong bounds on the oscillation parameters, excluding a large part of the region which could be relevant for the solar neutrinos [4]. In this region one expects the disappearance of the  $\nu_e$  flux due to conversion  $\nu_e \rightarrow \nu_\mu, \nu_\tau$  inside the star. It was marked however that oscillations inside the Earth can regenerate the  $\nu_e$  flux, so that the bound is absent in the region of the large mixing angle (LMA) solution of the solar neutrino problem [5, 6] (see also the discussions in [7, 8]). In this context, it was shown that the existence of the Earth matter effect depends on the conversion in the high density resonance associated with the large  $\Delta m^2$  which is responsible for the oscillations of atmospheric neutrinos [9, 10, 11]. In particular, the adiabatic conversion in the higher resonance suppresses the Earth matter effects associated with the lower  $\Delta m^2$  which governs solar neutrinos.

At the cooling stage, when the fluxes of all neutrino species are produced, the conversion inside the star leads to partial or complete permutation of the  $\bar{\nu}_e$  and  $\bar{\nu}_\mu, \bar{\nu}_\tau$  spectra [12, 13]. This causes the appearance of an high energy tail in the  $\bar{\nu}_e$  spectrum which

contradicts the SN1987A observations [13] and therefore implies the exclusion of some range of the large mixing angles. However in the range of  $\Delta m^2 \sim 10^{-5} \text{ eV}^2$  the bound is absent due to the Earth matter effect.

Further studies of the Earth matter effect on supernova neutrinos have been performed in ref. [14] in connection with the role the supernova neutrinos can play in the reconstruction of the neutrino mass spectrum. The three neutrino schemes both with normal and inverted mass hierarchy which explain the atmospheric and the solar neutrino data were considered. General formulas have been derived for neutrino and antineutrino fluxes at different detectors in presence of the Earth matter effect. The main qualitative features of the effect have been discussed and some examples of modification of the spectrum due to the Earth matter effect were given for schemes with LMA and SMA solutions of the solar neutrino problem. The role of the detection of the Earth matter effect in the identification of the neutrino mass scheme was clarified. In particular, it was shown that the very fact of the detection of the Earth matter effect in the neutrino and/or antineutrino channels will allow to establish the type of the mass hierarchy and to restrict the element  $U_{e3}$  of the mixing matrix.

In connection with the fact that the LMA gives the best global fit of the solar neutrino data, the interpretation of the SN1987A data has been revisited [15, 16, 17, 18]. The Earth matter effects on the antineutrino fluxes in the LMA range of the oscillation parameters have been studied in details (the two layer approximation of the Earth density profile has been used). The regions of the oscillation parameters have been found [16] in which the Earth matter effects can explain the difference of the K2 and IMB spectra. Such an interpretation also favors the normal mass hierarchy case or very small values of  $U_{e3}$  for the inverted mass hierarchy [19, 16, 17].

Recently, the Earth matter effects were considered also in ref. [20] where the expected spectra of events at SuperKamiokande (SK) and SNO have been calculated in three neutrino context with a two-layers approximation for the Earth profile.

In this paper we perform a detailed study of the Earth matter effect on the supernova neutrino fluxes in the three neutrino schemes which explain the solar and atmospheric neutrino data. Using the realistic Earth density profile, we study the dependence of the regeneration effect on the oscillation parameters, on the trajectory of the neutrinos inside the Earth and on the properties of the original neutrino fluxes. The effects are calculated for both neutrinos and antineutrinos.

We consider the possible arrival directions of the neutrino burst at existing detectors and estimate the probability to observe the Earth matter effect at least in two detectors. The possibility to identify the regeneration effect by existing and future experiments is discussed.

The paper is organized as follows. In section 2 we discuss the features of the neutrino fluxes originally produced in the star and the possible trajectories of the neutrinos inside the Earth. The general properties of the Earth matter effects are summarized in sect. 3; a more specific discussion for LMA oscillation parameters is given in sect. 4. In sect. 5 we briefly discuss the regeneration effects for neutrino parameters from the LOW and

SMA solutions of the solar neutrino problem. The possibilities of observation of the Earth matter effects are studied in sect. 6. Discussion and conclusions follow in sections 7 and 8.

## 2 From the star to the Earth: trajectories and spectra

### 2.1 Inside the star

In this section we summarize the features of the neutrino fluxes as they are produced inside the star and the properties of the supernova that will be used in our calculations.

A supernova is source of fluxes of neutrinos and antineutrinos of all the three flavours,  $e, \mu, \tau$ . These fluxes,  $F_\alpha^0$  and  $F_{\bar{\alpha}}^0$  ( $\alpha = e, \mu, \tau$ ), are characterized by the hierarchy of their average energies,

$$\langle E_e \rangle < \langle E_{\bar{e}} \rangle < \langle E_\mu \rangle , \quad (1)$$

and by the equality of fluxes of the non-electron neutrinos (which will be denoted as  $\nu_x$ ):

$$F_\mu^0 = F_{\bar{\mu}}^0 = F_\tau^0 = F_{\bar{\tau}}^0 \equiv F_x^0 . \quad (2)$$

In absence of neutrino mixing,  $\theta = 0$ , the neutrino flux at Earth is determined by the original flux produced in the star. If the decrease of the average energy and of the neutrino luminosity with time occurs over time scales larger than the duration of the burst the flux of the neutrinos of a given flavour,  $\nu_\alpha$ , can be described by a Fermi-Dirac spectrum as:

$$F_\alpha^0(E, T_\alpha, L_\alpha, D) = \frac{L_\alpha}{4\pi D^2 T_\alpha^4 F_3} \frac{E^2}{e^{E/T_\alpha} + 1} , \quad (3)$$

where  $E$  is the energy of the neutrinos,  $L_\alpha$  is the total energy released in  $\nu_\alpha$  and  $T_\alpha$  is the temperature of the  $\nu_\alpha$  gas in the neutrinosphere. Here  $D$  represents the distance of the supernova from the Earth; typically  $D \sim 10$  Kpc for a galactic supernova. The quantity  $F_3$  is given by  $F_3 = 7\pi^4/120 \simeq 5.68$ . According to the hierarchy (1) the indicative values  $T_e = 3.5$  MeV,  $T_{\bar{e}} = 5$  MeV and  $T_x = 8$  MeV will be taken as reference in our calculations; results will be presented also for other choices of the temperatures and their dependence on the specific values of  $T_e$ ,  $T_{\bar{e}}$  and  $T_x$  will be studied. We consider equipartition of the energy between the various flavours, so that  $L_\alpha \simeq E_B/6$ , with  $E_B$  the binding energy emitted in the core collapse of the star:  $E_B \simeq 3 \cdot 10^{53}$  ergs.

In presence of neutrino mixing and masses the neutrinos undergo flavour conversion on their way from the production point in the star to the detector at Earth. Matter effects dominate the conversion inside the star, where a wide range of matter densities is met. The conversion effects depend on the distribution of matter in the star; the radial profile

$$\rho_s(r) = 10^{13} C \left( \frac{10 \text{ Km}}{r} \right)^3 \text{ g} \cdot \text{cm}^{-3} , \quad (4)$$

with  $C \simeq 1 - 15$  provides a good description of the matter distribution for  $\rho_s \gtrsim 1 \text{ g} \cdot \text{cm}^{-3}$  [21, 8, 10, 22]. For  $\rho_s \lesssim 1 \text{ g} \cdot \text{cm}^{-3}$  the exact shape of the profile depends on the details of the composition of the star. For the neutrino parameters we will consider the resonant transitions in the star occur at densities larger than  $1 \text{ g} \cdot \text{cm}^{-3}$ , where the profile (4) applies; the value  $C = 4$  will be used unless differently stated.

## 2.2 Crossing the Earth

If the neutrinos cross the Earth before detection, regeneration effects can take place due to the interaction with the matter of the Earth, analogously to what is expected for solar neutrinos [23].

What is the chance that one, two or even three detectors situated in different places of the Earth will detect the Earth matter effect on supernova neutrinos?

Due to the short duration of the burst, and the spherical symmetry of the Earth, for a given detector the trajectories of neutrinos (and therefore the regeneration effect) can be completely described by the nadir angle  $\theta_n$  of the supernova with respect to the detector: if  $\cos \theta_n > 0$  the detector is shielded by the Earth. The angle  $\theta_n$  depends (i) on the location of the supernova in Galaxy, (ii) on the time  $t$  of the day at which the burst arrives at Earth and (iii) on the position of the detector itself.

We first consider a supernova located in the galactic center (declination<sup>1</sup>  $\delta_s = -28.9^\circ$ ) and three detectors [24]: LVD [25], SNO [26] and SK [27]. The positions of these detectors on the Earth are given in the Appendix A.

The fig. 1 a) shows the dependence of  $\cos \theta_n$  on the time  $t$  for the three detectors. We fixed  $t = 0$  to be the time at which the star lies on the Greenwich meridian. The horizontal line at  $\cos \theta_n = 0.83$  corresponds to the trajectory tangential to the core of the Earth ( $\theta_n = 33.2^\circ$ ), so that trajectories with  $\cos \theta_n < 0.83$  are in the mantle of the Earth. For  $\cos \theta_n > 0.83$  the trajectories cross both the mantle and the core.

From the figures it appears that:

1. For most of the arrival times the supernova is seen with substantially different nadir angles at the different detectors, so that one expects different Earth matter effects observed.
2. At any time  $t$  the neutrino signal arrives at Earth, at least one detector is shielded by the Earth ( $\cos \theta_n > 0$ ) and therefore will see the regeneration effect. Earth shielding is verified even for two detectors simultaneously for a large fraction of the times.
3. At any possible arrival time  $t$  one of the detectors is not shielded by the Earth. So that, once the direction to the supernova is known, one can identify such a detector and use its data to reconstruct the neutrino energy spectrum without regeneration effect.

---

<sup>1</sup>We define  $\delta_s$  as the the angle of the star with respect to the equatorial plane of the Earth.

4. For a substantial fraction of the times for one of the detectors the trajectory crosses the core of the Earth.

In fig. 1 b), c), we show similar dependences of  $\cos \theta_n$  on the time  $t$  for other locations of the star in the galactic plane. Notice that in the case b) two detectors are not shielded by the Earth for most of the times and no one trajectory crosses the core. In contrast, for the position c) all the three detectors are always shielded by the Earth. In general for the detectors we are considering, which are placed in the northern hemisphere, the Earth shielding is substantial for a supernova located in the southern hemisphere, as it is the case for stars in the region of the galactic center. If a supernova event occurs in the northern hemisphere ( $\delta_s > 0$ ), corresponding to some peripheral regions of the galactic disk, the Earth coverage of northern detectors will be scarce, or even null in the limit  $\delta_s = 90^\circ$ . In this case southern detectors would be more promising for the observation of Earth matter effects.

Clearly the determination of the position of the supernova is important for predictions and the experimental identification of the regeneration effect. The localization of the star can be done either by direct optical observations or by the experimental study of the neutrino scattering on electrons [28], which has substantial directionality. Triangulation techniques and neutron recoil methods have also been discussed [28, 29]. As we have mentioned in the Introduction, the study of Earth matter effects by high-statistics experiments can allow to reconstruct the direction to the star.

### 3 Neutrino conversion in the star and in the Earth

In this section we summarize the general properties of the Earth matter effect on supernova neutrinos. We will focus on the  $3\nu$ -schemes which explain the atmospheric and the solar neutrino data.

#### 3.1 Neutrino mass and mixing schemes

We assume that the atmospheric neutrinos have the dominant mode of oscillations  $\nu_\mu \leftrightarrow \nu_\tau$  with parameters [30]:

$$|m_3^2 - m_2^2| \equiv \Delta m_{atm}^2 = (1.5 - 4) \cdot 10^{-3} \text{eV}^2, \quad \sin^2 2\theta_{\mu\tau} > 0.88. \quad (5)$$

The solar neutrino data are explained either by vacuum oscillations (VO solution) or by one of the MSW solutions (LMA, SMA or LOW). The latter are based on the resonant conversion driven by the oscillation parameters

$$|m_2^2 - m_1^2| \equiv \Delta m_\odot^2, \quad \sin^2 2\theta_\odot. \quad (6)$$

Moreover, we consider  $\Delta m_{atm}^2 \gg \Delta m_\odot^2$ .

The electron flavor is distributed in the mass eigenstates  $\nu_1$  and  $\nu_2$  with admixtures  $U_{e1} \approx \cos \theta_\odot$ ,  $U_{e2} \approx \sin \theta_\odot$ . We will call  $\nu_1$  and  $\nu_2$  the solar pair of states.

Three features of the neutrino schemes, which are important for the supernova neutrino conversion, are still unknown:

1. The admixture  $U_{e3}$  of the  $\nu_e$  in the third eigenstate. Only an upper bound on this parameter is known from the CHOOZ and Palo Verde experiments [31, 32]:

$$|U_{e3}|^2 \lesssim 0.02 . \quad (7)$$

2. The type of mass hierarchy. In the case of *normal* mass hierarchy the solar pair of states is lighter than  $\nu_3$ :  $m_3 > m_2, m_1$ . In the case of inverted mass hierarchy the states of the solar pair are heavier than  $\nu_3$ :  $m_3 < m_2 \approx m_1$ .
3. The values of the solar parameters  $\Delta m_{\odot}^2$ ,  $\sin^2 2\theta_{\odot}$ . Different solutions correspond to substantially different values of the oscillation parameters (see e.g. [33]).

The masses and mixings determine the pattern of level crossings in the star [14]. There are two resonances (level crossings) in the schemes under consideration:

- The high density (H) resonance, determined by the parameters  $\Delta m_{atm}^2$  and  $U_{e3}$ . The conversion in the region of this resonance is described by the Landau-Zener type probability,  $P_H$ , of transition between the mass eigenstates  $\nu_2$  and  $\nu_3$ .
- The low density (L) resonance with parameters of the solar pair:  $\Delta m_{\odot}^2$ ,  $\sin^2 2\theta_{\odot}$ . We denote as  $P_L$  the probability of  $\nu_2 \rightarrow \nu_1$  transition associated to this resonance.

Depending on the type of mass hierarchy and on the value of  $\theta_{\odot}$ , the resonances appear in different channels. There are four possibilities [14]:

1. normal mass hierarchy and  $\theta_{\odot} < \pi/4$ : both the resonances are in the neutrino channel.
2. normal mass hierarchy and  $\theta_{\odot} > \pi/4$ : the H resonance is in the neutrino channel, whereas the L resonance is in the antineutrino channel. This possibility is disfavored by the present data on solar neutrinos.
3. inverted mass hierarchy and  $\theta_{\odot} < \pi/4$ : the H resonance is in the antineutrino channel, the L resonance is in the neutrino channel.
4. inverted mass hierarchy and  $\theta_{\odot} > \pi/4$ : both the resonances are in the antineutrino channel.

These different schemes correspond to different conversion effects both inside the star and in the matter of the Earth. As it was shown in [14], the Earth effects in the  $3\nu$  context depend on (i) the type of mass hierarchy, (ii) the adiabaticity in the high density resonance, which is determined by  $|U_{e3}|$  and by the density profile of the star, (iii) the

oscillation parameters in the low resonance which are determined by the solution of the solar neutrino problem.

In what follows we will consider the various possibilities in order. We will take oscillation parameters from one of the regions of the solutions of the solar neutrino problem, and also assume that the mixing parameter  $|U_{e3}|$  is small, so that oscillations inside the Earth are reduced to  $2\nu$  problem.

### 3.2 Antineutrino channels

Let us first consider the scheme with normal mass hierarchy.

As discussed in sect. 3.1, in this case there is no level crossing in the high resonance region in the antineutrino channel, so that the antineutrino flux at the detector does not depend on the jump probability  $P_H$ . We get:

$$F_{\bar{e}}^D = F_{\bar{e}} + (F_{\bar{e}}^0 - F_x^0)(1 - 2\bar{P}_L)(\bar{P}_{1e} - |U_{e1}|^2) , \quad (8)$$

where

$$F_{\bar{e}} \approx F_{\bar{e}}^0 - (F_{\bar{e}}^0 - F_x^0)[(1 - \bar{P}_L) - (1 - 2\bar{P}_L)|U_{e1}|^2] \quad (9)$$

is the  $\bar{\nu}_e$  flux arriving at the surface of the Earth (without Earth matter effect) and the fluxes  $F_{\alpha}^0$  are defined in eq. (3). Here  $\bar{P}_{1e}$  denotes the probability of  $\bar{\nu}_1 \rightarrow \bar{\nu}_e$  conversion inside the Earth and  $\bar{P}_L$  is the jump probability in the L resonance. The forms (8)-(9) are the consequence of the approximate factorization of the dynamics and reduction of the three neutrino problem to an effective two neutrino conversion (see [14] for details).

Let us consider the relative Earth effect expressed by the ratio:

$$\bar{R} \equiv \frac{F_{\bar{e}}^D - F_{\bar{e}}}{F_{\bar{e}}} . \quad (10)$$

From eqs. (8)-(9) we find

$$\bar{R} = \bar{r}(1 - 2\bar{P}_L)\bar{f}_{reg} , \quad (11)$$

where  $\bar{r}$  is the (“reduced”) flux factor:

$$\bar{r} \equiv \frac{F_{\bar{e}}^0 - F_x^0}{F_{\bar{e}}^0 [\bar{P}_L + (1 - 2\bar{P}_L)|U_{e1}|^2] + F_x^0 [(1 - \bar{P}_L) - (1 - 2\bar{P}_L)|U_{e1}|^2]} , \quad (12)$$

and  $\bar{f}_{reg}$  the regeneration factor:

$$\bar{f}_{reg} \equiv (\bar{P}_{1e} - |U_{e1}|^2) . \quad (13)$$

The three factors present in eq. (11) describe the initial conditions (initial fluxes) and different stages of the evolution of the antineutrino state. Let us consider the properties of these factors in order.



1. The **L-resonance factor**,  $(1 - 2\bar{P}_L)$ , is close to the adiabatic value 1 (i.e.  $\bar{P}_L \simeq 0$ ) especially if the resonance is in the neutrino channel [34]. So, in this case from eqs. (11)-(12) we get the simplified expressions:

$$\bar{R} = \bar{r}\bar{f}_{reg} , \quad (14)$$

$$\bar{r} = \frac{F_e^0 - F_x^0}{F_e^0|U_{e1}|^2 + F_x^0(1 - |U_{e1}|^2)} . \quad (15)$$

2. The **flux factor**, eq. (15), determines the sign and the size of the effect. Due to the hierarchy of energies, eq. (1), a critical energy  $\bar{E}_c$  exists at which  $\bar{r} = 0$ . Furthermore we have  $\bar{r} > 0$  below the critical energy,  $E < \bar{E}_c$ , and  $\bar{r} < 0$  for  $E > \bar{E}_c$ . For realistic temperatures of the neutrino fluxes (see sect. 2.1) one gets:

$$\bar{E}_c = (25 - 28) \text{ MeV} . \quad (16)$$

At  $E \gg \bar{E}_c$  the flux factor (15) is dominated by the harder flux  $F_x^0$ , so that one finds the asymptotic behavior:

$$\bar{r}(E \gg \bar{E}_c) = -\frac{1}{(1 - |U_{e1}|^2)} \simeq -\frac{1}{|U_{e2}|^2} . \quad (17)$$

Similarly, at  $E \ll \bar{E}_c$  the flux  $F_e^0$  dominates, giving the limit:

$$\bar{r}(E \ll \bar{E}_c) = \frac{1}{|U_{e1}|^2} . \quad (18)$$

From eqs. (17)-(18) it follows that at very high, as well as at very low energies, the relative regeneration effect (14) becomes independent of the original fluxes.

3. The **regeneration factor**, eq. (13), describes the propagation effect inside the Earth and is analogous to the regeneration factor which appears for solar neutrinos. Notice that  $\bar{f}_{reg}$  corresponds to genuine matter effect: it is zero in vacuum.

The dynamics of propagation and properties of the regeneration factor (13) are different for oscillation parameters from different solutions of the solar neutrino problem.

In what follows we perform numerical calculations of the Earth regeneration factor using a realistic density profile of the Earth [35]. We compare these results with results of the two layers approximation in the Appendix B.

### 3.3 Neutrino channels

If the hierarchy of the neutrino mass spectrum is normal, the H resonance is in the neutrino channel and the  $\nu_e$  flux at the detector depends on  $P_H$  [14]:

$$F_e^D \simeq F_e + (F_e^0 - F_x^0)P_H(1 - 2P_L)(P_{2e} - |U_{e2}|^2) , \quad (19)$$

where the  $\nu_e$  flux arriving at the surface of the Earth equals:

$$F_e \simeq F_e^0 - (F_e^0 - F_x^0)[1 - P_H P_L - P_H(1 - 2P_L)|U_{e2}|^2] . \quad (20)$$

Here  $P_{2e}$  is the probability of the transition  $\nu_2 \rightarrow \nu_e$  inside the Earth.

From eqs. (19)-(20) one finds the relative Earth matter effect,  $R \equiv (F_e^D - F_e)/F_e$ , and the flux factor,  $r$ :

$$R = r P_H (1 - 2P_L) f_{reg} , \quad (21)$$

$$r = \frac{F_e^0 - F_x^0}{F_e^0 P_H [P_L + (1 - 2P_L)|U_{e2}|^2] + F_x^0 [1 - P_H P_L - P_H(1 - 2P_L)|U_{e2}|^2]} . \quad (22)$$

The regeneration factor,  $f_{reg}$ , is given by:

$$f_{reg} \equiv (P_{e2} - |U_{e2}|^2) = -(P_{1e} - |U_{e1}|^2) . \quad (23)$$

Let us comment on the features of the ratio  $R$ :

1. From eq. (21) it follows that if the adiabaticity in the high density (H) resonance inside the star is fulfilled,  $P_H \rightarrow 0$ , the Earth matter effect disappears. The reason is that in the adiabatic case the original electron neutrinos convert almost completely into  $\nu_\mu$  and  $\nu_\tau$  fluxes in the H resonance. Then the electron neutrinos detected at Earth result from the conversion of the original  $\nu_\mu$  and  $\nu_\tau$  fluxes. Since these fluxes are equal, eq. (2), no oscillation effect will be observed due to conversion in the low density resonance.

The Earth matter effect is maximal in the limit of strong violation of the adiabaticity in the H-resonance:  $P_H \rightarrow 1$ , when the dynamics is reduced to a two neutrino problem with oscillation parameters of the L resonance.

The jump probability  $P_H$  is determined by the density profile of the star and the oscillation parameters  $|U_{e3}|^2 \approx \tan^2 \theta_{13}$  and  $\Delta m_{atm}^2$ . In fig. 2 we show the lines of equal  $P_H$  in the  $(\Delta m_{atm}^2 - \tan^2 \theta_{13})$ - plane, together with the exclusion region from the CHOOZ experiment. We use the density profile (4); the error in  $P_H$  due to the uncertainty in the density profile is estimated to be within a factor of 2 [14]. The figure shows that as  $|U_{e3}|^2$  decreases in the range allowed by the bound (7) the transition in the H resonance varies from perfectly adiabatic ( $P_H \simeq 0$ ), for  $|U_{e3}|^2 \gtrsim 5 \cdot 10^{-4}$ , to strongly non-adiabatic ( $P_H \simeq 1$ ), for  $|U_{e3}|^2 \lesssim 10^{-6}$ . The intervals of adiabaticity and strong adiabaticity violation change only mildly as  $\Delta m_{atm}^2$  varies in the presently allowed range. Notice that future atmospheric neutrino studies and the long base-line experiments will sharpen the allowed region of  $\Delta m_{atm}^2$ .

2. The low density resonance factor,  $(1 - 2P_L)$ , is zero if  $P_L = 1/2$ , which corresponds to a situation when the neutrino beam arriving at Earth consists in incoherent and equal fluxes of  $\nu_1$  and  $\nu_2$ . In this case the effects of  $\nu_1 \rightarrow \nu_e$  and  $\nu_2 \rightarrow \nu_e$  oscillations cancel each other.

In fig. 3 we show the lines of  $P_L = 1/2$ , calculated with the density profile (4) in the  $(\tan^2 \theta_\odot - \Delta m_\odot^2)$  plane for different values of the neutrino energy. The lines cross the

allowed region of the SMA solutions for the energy interval  $E = 5 - 15$  MeV. In fig. 3 we show also the lines  $P_L = 0.05$  for two different energies:  $E = 5$  MeV and  $E = 50$  MeV. These lines determine the lower edge of the adiabaticity region in the  $(\tan^2 \theta_\odot - \Delta m_\odot^2)$  plane. Notice that the LMA region is in the adiabaticity domain for all the relevant energies, whereas the SMA solution region is in the domain of significant adiabaticity violation. Depending on the details of the density profile of the star the LOW solution lies either in the adiabaticity region or in the region of partial adiabaticity breaking.

A qualitative treatment does not depend on whether the low density resonance is in the neutrino or antineutrino channel (dark side of the parameter space). Quantitatively the results are different.

3. The flux factor,  $r$ , eq. (22), changes sign at lower critical energy with respect to the case of antineutrinos, since the original  $\nu_e$  spectrum is softer than the  $\bar{\nu}_e$  spectrum. We get:

$$E_c = (16 - 24) \text{ MeV} . \quad (24)$$

Similarly to what was discussed for  $\bar{\nu}_e$ , the flux factor becomes independent of the original fluxes in the low and high energy limits:

$$r(E \gg E_c) = -\frac{1}{1 - P_H P_L - P_H(1 - 2P_L)|U_{e2}|^2} , \quad (25)$$

$$r(E \ll E_c) = \frac{1}{P_H [P_L + (1 - 2P_L)|U_{e2}|^2]} . \quad (26)$$

4. The Earth regeneration factor, eq. (23), depends on the mixing and mass squared difference of the solar pair and on the nadir angle  $\theta_n$ . It will be described in detail in the following sections.

### 3.4 Schemes with inverted mass hierarchy

If the hierarchy of the mass spectrum is inverted the high density resonance is in the antineutrino channel (see sect. 3.1) and the Earth matter effect for  $\bar{\nu}_e$  depends on the jump probability  $P_H$ . The expressions (8)-(9) for the  $\bar{\nu}_e$  fluxes are immediately generalized to:

$$F_{\bar{e}}^D = F_{\bar{e}} + (F_{\bar{e}}^0 - F_x^0)P_H(1 - 2\bar{P}_L)(\bar{P}_{1e} - |U_{e1}|^2) , \quad (27)$$

$$F_{\bar{e}} \approx F_{\bar{e}}^0 - (F_{\bar{e}}^0 - F_x^0)[1 - P_H\bar{P}_L - P_H(1 - 2\bar{P}_L)|U_{e1}|^2] , \quad (28)$$

in analogy with eqs. (19)-(20).

Taking  $\bar{P}_L = 0$  (see sect. 3.2), we find the relative deviation,  $\bar{R}$ , and the reduced flux factor:

$$\bar{R} = \bar{r}P_H\bar{f}_{reg} , \quad (29)$$

$$\bar{r} = \frac{F_{\bar{e}}^0 - F_x^0}{F_{\bar{e}}^0 P_H |U_{e1}|^2 + F_x^0 (1 - P_H |U_{e1}|^2)} , \quad (30)$$

with the asymptotic limits:

$$\bar{r}(E \gg \bar{E}_c) = -\frac{1}{1 - P_H |U_{e1}|^2}, \quad (31)$$

$$\bar{r}(E \ll \bar{E}_c) = \frac{1}{P_H |U_{e1}|^2}. \quad (32)$$

Clearly, the conversion of  $\nu_e$  is independent of  $P_H$ . The expressions of the neutrino fluxes  $F_e^D$  and  $F_e$  can be obtained from eqs. (19)-(20) by the replacement  $P_H \rightarrow 1$ ; they become analogous to eqs. (8)-(9). With the same prescription, from eqs. (21)-(22) one gets the expressions of the ratios  $R$  and  $r$ .

Summarizing the results of sections 3.2-3.4 we can say that the mass hierarchy and the adiabaticity in the H density resonance (and thus  $U_{e3}$ ) determine the channel ( $\nu_e$  or  $\bar{\nu}_e$ ) in which the Earth matter effects appear, which is:

- both the  $\nu_e$  and  $\bar{\nu}_e$  channels if the H resonance is strongly non-adiabatic,  $P_H = 1$ , regardless to the hierarchy.
- the  $\bar{\nu}_e$  channel for adiabatic H resonance,  $P_H = 0$ , and normal hierarchy.
- the  $\nu_e$  channel for adiabatic H resonance,  $P_H = 0$ , and inverted hierarchy.

The possibility of probing  $U_{e3}$  and the mass hierarchy by the study of Earth effects on supernova neutrinos will be discussed in sect. 7.

## 4 The Earth matter effects for the LMA parameters

### 4.1 Antineutrino channels

Let us now study the features of the relative Earth matter effect, eq. (14), for  $\bar{\nu}_e$  with mixing and mass squared difference in the LMA region.

The dynamics of the conversion inside the Earth is described by the regeneration factor  $\bar{f}_{reg}$ , eq. (13). For LMA parameters the Earth matter effect consists in an oscillatory modulation of the neutrino energy spectrum.

The fig. 4 shows the ratio  $\bar{R}$  as a function of the neutrino energy for various values of  $\theta_n$ . For mantle crossing trajectories,  $\theta_n > 33.2^\circ$ , the effect is mainly due to the interplay of oscillations and adiabatic evolution. That is, oscillations in medium with slowly varying density. Small density jumps produce only rather weak effects. As a result, the features of the regeneration factor,  $\bar{f}_{reg}$ , are similar to what is predicted in the case of propagation in medium with constant density (see Appendix B). The factor is positive in the whole energy spectrum, so that the sign of the matter effect is determined by the flux factor (15): we have  $\bar{R} > 0$  for  $E < \bar{E}_c$  and  $\bar{R} < 0$  for  $E > \bar{E}_c$ .

The energy spectrum shows regular oscillations in energy with period

$$\Delta E \approx \frac{2\pi}{\phi(\theta_n, E)} E, \quad (33)$$

where the oscillation phase  $\phi$  is determined by the integral

$$\phi(\theta_n) = 2\pi \int_0^{r(\theta_n)} \frac{dx}{l_m(n(x), E)} \quad (34)$$

over the neutrino trajectory. Here  $l_m$  is the (instantaneous) oscillation length in matter, and  $n(x)$  is the electron density along the trajectory. As follows from eqs. (33)-(34) the period of oscillations decreases with the nadir angle and increases with the energy. The dependence on the energy appears in  $\Delta E$ , (see eq. (33)) explicitly, and implicitly via the oscillation length.

As a result of adiabatic evolution, the depth of oscillations of the regeneration factor is determined by the electron number density at the surface of the Earth (see Appendix B),  $n_e^0$ :

$$\bar{D}_f \approx 2\sqrt{2}G_F n_e^0 \frac{E}{\Delta m_\odot^2} \sin^2 2\theta_m^0. \quad (35)$$

Here  $\theta_m^0$  is the mixing angle of the solar pair in matter at the surface.

The depth  $\bar{D}_f$  has a resonant dependence on the quantity  $x \equiv 2E|V|/\Delta m_\odot^2$ , with  $V$  being the matter potential (see the Appendix B for details). Both  $\bar{D}_f$  and  $l_m$  increase as the system approaches the resonance; correspondingly, the period  $\Delta E/E$  increases. For neutrinos propagating in the mantle and  $\Delta m_\odot^2 = 5 \cdot 10^{-5} \text{ eV}^2$  (which is used in the figure 4) the resonance is realized at  $E = E_R \simeq 150 \text{ MeV}$ . Thus the Earth effect is larger in the highest energy part of the spectrum.

For core crossing trajectories the behavior of the Earth effect becomes irregular due to the interference of the oscillations in the core and in the mantle. The modulations in the energy spectra have smaller period both due to presence of large densities and larger length of the trajectory. Moreover, now the effect can change the sign both below and above the critical energy. That is, for some energies the Earth effect is negative at low energies and positive at high energies.

As  $\Delta m_\odot^2$  decreases, as shown in fig. 5, the regeneration factor increases, since the resonance of the system is realized at lower energies. In particular, for  $\Delta m_\odot^2 = 2 \cdot 10^{-5} \text{ eV}^2$ , the resonance energy equals  $E_R \simeq 60 \text{ MeV}$ . The period (in the energy scale) of the oscillatory modulation of the spectrum increases with the decrease of  $\Delta m_\odot^2$ .

The change of the mixing parameter  $|U_{e1}|^2 \approx \cos^2 \theta_\odot$  (within the LMA region) influences the regeneration factor rather weakly. However variations of  $|U_{e1}|^2$  change the spectrum arriving at the surface of the Earth. According to the eq. (9), with the increase of  $|U_{e1}|^2$  (i.e. decrease of the mixing  $\theta_\odot$ ), the contribution of the hard component in the spectrum decreases: the composite spectrum becomes softer.

Given the mixing  $U_{e1}$  the factor  $\bar{r}$ , eq. (15), depends only on the original fluxes,  $F_e^0$  and  $F_x^0$ . The fig. 6 shows the relative Earth effect,  $\bar{R}$ , as a function of the energy for different

values of  $\bar{r}$  determined by different temperatures of the original  $\bar{\nu}_e$  spectrum. As it appears in the figure, the critical energy  $\bar{E}_c$  decreases with  $T_{\bar{e}}$ , so that the region in which the flux factor suppresses the regeneration effect shifts to lower energies. For  $E \ll \bar{E}_c$  and  $E \gg \bar{E}_c$  the depth of oscillations depends only very weakly on variations of  $T_{\bar{e}}$ , according to the limits (18) and (17), which do not depend on temperatures. The values of  $T_{\bar{e}}$  and  $T_x$  only affect the rapidity of the convergence to these limits: the convergence is faster for the larger difference  $T_x - T_{\bar{e}}$ . This appears in fig. 7 b), in which the flux factor  $\bar{r}$  is plotted as a function of the antineutrino energy with the same parameters as in the fig. 6. For  $\sin^2 2\theta_{\odot} = 0.75$ , as used in the figs. 6-7, one finds  $\bar{r}(E \ll \bar{E}_c) = 1.33$  and  $\bar{r}(E \gg \bar{E}_c) = -4$ . Thus the Earth effect has stronger enhancement at high energies.

If the hierarchy is inverted the Earth matter effect on  $\bar{\nu}_e$  is affected by the adiabaticity in the high density resonance. Such dependence is illustrated in fig. 8, which shows the relative effect  $\bar{R}$  as a function of the energy for various values of  $P_H$ . According to eq. (29) the effect is proportional to  $P_H$  and is maximal at  $P_H = 1$ . The dependence of  $\bar{R}$  on  $P_H$  is transparent in the limits of high and low energies. Combining eqs. (29) and (31) we find that at high energies  $\bar{R}$  depends on  $P_H$  as:

$$\bar{R}(E \gg \bar{E}_c) = -\frac{P_H}{1 - P_H|U_{e1}|^2} \bar{f}_{reg} , \quad (36)$$

that is,  $\bar{R} \propto P_H$  for  $P_H \ll 1$ . The weak dependence of  $\bar{R}$  on  $P_H$  in the softer part of the spectrum in fig. 8 is explained by the fact that the dependence on  $P_H$  cancels in the low energy limit,  $E \ll \bar{E}_c$ , as can be seen from eqs. (29) and (32).

## 4.2 Neutrino channels

Let us discuss the properties of the Earth regeneration effect in the  $\nu_e$  channel.

As it was shown in fig. 3, for LMA oscillation parameters the adiabaticity in the L-resonance inside the star is satisfied, so that  $P_L = 0$  and eqs. (21)-(22) reduce to:

$$R = r P_H f_{reg} , \quad (37)$$

$$r = \frac{F_e^0 - F_x^0}{F_e^0 P_H |U_{e2}|^2 + F_x^0 (1 - P_H |U_{e2}|^2)} . \quad (38)$$

The regeneration factor  $f_{reg}$ , eq. (23), and therefore  $R$ , have similar dependence on  $\theta_n$  and  $\Delta m_{\odot}^2$  as in the case of antineutrinos. These dependences are illustrated in the figs. 9 and 10, where  $P_H = 1$  was taken. The oscillation length and the period of the modulations in the energy spectrum increase with the increase of the energy and the decrease of  $\Delta m_{\odot}^2$  (fig. 10). The depth of the oscillations of the regeneration factor  $f_{reg}$  is larger than for antineutrinos since (if the L resonance is in the neutrino channel) matter enhances the  $\nu_e$  mixing and suppresses the mixing of  $\bar{\nu}_e$  :

$$\sin^2 2\theta_m(\bar{\nu}) < \sin^2 2\theta_{\odot} < \sin^2 2\theta_m(\nu) . \quad (39)$$

The depth of oscillations has a resonant character (see Appendix B), increasing as the resonance energy is approached. According to eq. (35) the depth gets larger for smaller  $\Delta m_{\odot}^2$  (fig. 10).

The dependence of the Earth matter effect on the flux factor,  $r$ , eq. (38), is illustrated in fig. 11, where the ratio  $R$  is plotted for different values of the temperature  $T_e$ ,  $T_x = 8$  MeV and  $P_H = 1$ . According to sects. 3.2 and 3.3 the flux factor suppresses the Earth matter effect at energies close to the critical energy,  $E_c$ , which is slightly lower than for  $\bar{\nu}_e$ :  $E_c \simeq 22$  MeV for  $T_e = 3.5$  MeV. At high and low energies the asymptotic limits (25)-(26) are realized. This is shown in fig. 7 a), with the same values of the temperatures as in fig. 11 and  $P_H = 1$ . From eqs. (25)-(26) (with  $P_L = 0$ ) and from the fig. 7 it follows that, in contrast to the case of  $\bar{\nu}_e$ , the Earth effect has stronger enhancement at low energy: for  $\sin^2 2\theta_{\odot} = 0.75$  one gets  $r(E \ll E_c) = 4$  and  $r(E \gg E_c) = -1.33$ . Notice that the convergence to these limits is faster than for  $\bar{\nu}_e$  due to larger difference of the  $\nu_e$  and  $\nu_x$  temperatures.

According to eq. (37), the Earth matter effect is larger for larger  $P_H$ , i.e. for maximal adiabaticity breaking in the high density resonance inside the star. From eqs. (37) and (38) the following asymptotic limit follows:

$$R(E \gg E_c) = -\frac{P_H}{1 - P_H|U_{e2}|^2} f_{reg}, \quad (40)$$

similarly to eq. (36). The combination of eqs. (37) and (26) implies that  $R$  becomes independent of  $P_H$  at  $E \ll E_c$ . These features of the dependence of  $R$  on  $P_H$  are shown in fig. 12.

As discussed in sect. 3.4, the results for inverted hierarchy of the spectrum are obtained from the description given for normal hierarchy by the replacement  $P_H \rightarrow 1$ . Therefore the results shown in the figs. 9-11, in which  $P_H = 1$  was used, apply to the case of inverted hierarchy.

## 5 The case of oscillation parameters in the LOW and SMA regions

### 5.1 LOW parameters

For oscillation parameters in the region of the LOW solution of the solar neutrino problem the mass squared difference is smaller by at least two orders of magnitude with respect to the LMA solution:  $\Delta m_{\odot}^2 \sim 10^{-8} - 10^{-7} \text{ eV}^2$ . Therefore the resonance energy in the Earth is very small,  $E_R < 1$  MeV, and in the whole energy spectrum of supernova neutrinos the neutrino system is far above the resonance. Both the  $\nu_e$  and  $\bar{\nu}_e$  mixings are suppressed in the matter of the Earth and the oscillation lengths approach the refraction length,

$l_m \approx l_0 \sim 8000$  Km. As a consequence, the regeneration inside the Earth has only weak dependence on the neutrino energy and no oscillatory distortions appear in the energy spectra at the detectors. In contrast, the regeneration effect depends strongly on the nadir angle  $\theta_n$ : for  $E = 10$  MeV the regeneration factor has a maximum,  $f_{reg} \simeq 0.04$ , for  $\theta_n \simeq 25^\circ$  (see e.g. [36]).

The fig. 13 shows the relative Earth effects for  $\nu_e$  and  $\bar{\nu}_e$  as functions of the energy for  $\Delta m_\odot^2 = 10^{-7}$  eV<sup>2</sup>,  $\sin^2 2\theta_\odot = 0.9$ ,  $\theta_n = 25^\circ$  and  $P_H = 1$ . We have also considered perfect adiabaticity in the L resonance inside the star,  $P_L = 0$ . The figure shows that for  $E > 5$  MeV the effect is not larger than 20% for  $\nu_e$  and 10% for  $\bar{\nu}_e$ ; it decreases with the increase of energy with a  $\sim 1/E$  behavior. In the neutrino channel the relative deviation  $R$ , eq. (21), is larger than in the antineutrino channel, especially in the very soft part of the spectrum,  $E \lesssim 10$  MeV. This is explained (i) by the fact that the neutrino system approaches the resonance at low energies, and therefore the  $\nu_e$  mixing is enhanced, and (ii) by the larger flux factor in the low energy limit,  $E \ll E_c$  (see fig. 7). We get  $\sim 50\%$  effect at  $E = 2$  MeV and  $\sim 100\%$  at  $E = 1$  MeV.

## 5.2 SMA parameters

For oscillation parameters in the SMA region the fluxes at the detector,  $F_e^D$  and  $F_{\bar{e}}^D$ , eqs. (8) and (19), are substantially different with respect to the case of LMA parameters, due to differences in the L resonance factor,  $(1 - 2P_L)$ , and in the regeneration factor.

In what follows we describe the Earth effect for  $\nu_e$ ; effects on  $\bar{\nu}_e$  conversion are extremely small due to the suppression of the mixing in matter and will not be considered.

Let us first discuss the factor  $(1 - 2P_L)$ . For  $\Delta m_\odot^2$  and  $\sin^2 2\theta_\odot$  in the SMA region the conversion in the L resonance inside the star occurs in the adiabaticity breaking regime (fig. 3). The jump probability  $P_L$  differs from 0 significantly and, in particular, as shown in fig. 3,  $P_L$  is close to 1/2, thus suppressing the matter effect (eq. (21)).

In fig. 14 we show the factor  $(1 - 2P_L)$  as a function of the neutrino energy for  $\Delta m_\odot^2 = 6 \cdot 10^{-6}$  eV<sup>2</sup> and two values of  $\sin^2 2\theta_\odot$  in the SMA region. We used the profile (4) with  $C = 4$ . For the largest possible mixing,  $\sin^2 2\theta_\odot \sim 5 \cdot 10^{-3}$ , the factor is negative above 10 MeV; for the best fit point,  $\sin^2 2\theta_\odot \sim 2.4 \cdot 10^{-3}$ , it is negative in the whole detectable part of the spectrum ( $E > 5$  MeV). These results, however, strongly depend on the model of the star. For massive stars ( $M > 30M_\odot$ ) the density profile may have smaller gradient, so that the adiabaticity breaking is weaker. In this case the energy at which  $P_L = 1/2$  is larger, and in a significant part of the spectrum the low resonance factor can be positive. Notice that in the high energy part of the spectrum the factor can be as large as 0.7 - 0.8 in absolute value.

The regeneration factor,  $f_{reg}$ , eq. (23), has a peculiar resonant behaviour in dependence on the energy and on the nadir angle  $\theta_n$ . For mantle crossing trajectories,  $\theta_n > 33.2^\circ$ , the matter effect consists in resonantly enhanced oscillations, with oscillation length comparable or larger than the radius of the Earth. A peak appears in the  $\nu_e$  spectrum at  $E \sim 15$



MeV.

For core crossing trajectories,  $\theta_n < 33.2^\circ$ , the regeneration factor exhibits a narrow peak at  $E \simeq 7$  MeV due to parametric resonance, with two smaller peaks at higher and lower energy due to MSW resonances in the mantle and in the core respectively. These features are shown in the fig. 15, which represents the relative deviation  $R$  as a function of the energy for  $P_H = 1$ ,  $\theta_n = 0^\circ$  and various values of the factor  $C$  in the density profile (4), corresponding to different values of  $P_L$ . With increase of  $C$  the jump probability  $P_L$  decreases, so that the region where  $(1 - 2P_L) > 0$  expands to higher energies. With the decrease of  $P_L$  the Earth matter effect changes from negative to positive and the size of the effect increases; it can be as large as  $\sim 30\%$ .

As in the case of the LMA solution, the effect decreases with  $P_H$  and disappears for perfectly adiabatic transition in the H resonance,  $P_H = 0$ . If the mass hierarchy is inverted the matter effect exists, in the neutrino channel, independently of the character of the H resonance.

## 6 Observation of Earth effects

Let us first summarize the results of the previous sections.

The regeneration effects in the matter of the Earth produce a distortion of the neutrino energy spectrum. The character of the distortion depends (i) on the properties of the original neutrino and antineutrino fluxes, (ii) on the nadir angle  $\theta_n$  and (iii) on the features of the neutrino masses and mixings, in particular on the solution of the solar neutrino problem.

For oscillation parameters from the LMA solution the distortion of the spectrum has oscillatory character with larger oscillation depth and period in the high energy part of the spectrum. The effect exists in the neutrino or in the antineutrino channel or in both depending on the adiabaticity in the H resonance and on the mass hierarchy.

For the LOW solution there is no oscillatory behaviour in the spectra. The effect is very small in the whole observable part of the energy spectrum and decreases with the increase of the energy.

For parameters in the region of the SMA solution the Earth effect exists for neutrinos only and consists in the appearance of one or three (for core crossing trajectories) resonance peaks (or dips) in the low energy part of the spectrum.

In this section we discuss the possibility of detecting the Earth matter effects at present and future detectors.

### 6.1 Detection of supernova neutrinos. Numbers of events

As follows from the results of the previous sections, the observation of the Earth matter effect requires: (i) separate detection of neutrinos of different flavours, (ii) separate detection of neutrinos and antineutrinos, (iii) the reconstruction of the neutrino energy spectrum.

In what follows we concentrate on events from charged current (CC) scattering on nucleons or nuclei at real-time detectors. These events better satisfy the requirements (i)-(iii); in particular CC processes have high sensitivity to the neutrino energy spectrum.

We consider:

1. The detection of  $\bar{\nu}_e$  at water Cerenkov detectors (SuperKamiokande and the outer volume of SNO) via the reaction:

$$\bar{\nu}_e + p \rightarrow e^+ + n . \quad (41)$$

Other CC reactions (e.g. the scattering of  $\nu_e$  and  $\bar{\nu}_e$  on oxygen nuclei) have substantially smaller cross section so that they contribute to the total number of events at few per cent level; they will not be considered further.

2. Heavy water detectors (the inner volume of SNO experiment) with the detection reactions:

$$\nu_e + d \rightarrow e + p + p , \quad (42)$$

$$\bar{\nu}_e + d \rightarrow e^+ + n + n , \quad (43)$$

which represent the dominant channel of CC detection. Events from the process (43) will be distinguished by those from (42) if neutrons are efficiently detected in correlation with the positron.

3. Liquid scintillator detectors (LVD), which are mostly sensitive to  $\bar{\nu}_e$  via the reaction (41) with only little sensitivity to absorption processes on carbon nuclei.

Besides pure CC processes, the reactions

$$\nu_i + e \rightarrow \nu_i + e , \quad i = e, \mu, \tau, \quad (44)$$

$$\bar{\nu}_i + e \rightarrow \bar{\nu}_i + e , \quad (45)$$

and the NC breakup of deuterium:

$$\nu_i + d \rightarrow \nu_i + n + p , \quad i = e, \mu, \tau, \quad (46)$$

$$\bar{\nu}_i + d \rightarrow \bar{\nu}_i + n + p , \quad (47)$$

allow to reconstruct the total neutrino flux; moreover, due to its good directionality, the scattering of  $\nu_e$  on electrons is relevant to the location of the supernova.

Radiochemical experiments could provide information on the total  $\nu_e$  flux above a certain threshold.

The number of CC events with lepton having the observed kinetic energy  $E_e$  is given by

$$\frac{dN_\alpha}{dE_e} = N_T \int_{-\infty}^{+\infty} dE'_e R(E_e, E'_e) \mathcal{E}(E'_e) \int dE F_\alpha(E) \frac{\sigma(E'_e, E)}{dE'_e} , \quad (48)$$

where  $E'_e$  is the true energy of the electron (or positron),  $N_T$  is the number of target particles in the fiducial volume and  $\mathcal{E}$  represents the detection efficiency. Here  $\sigma(E'_e, E)/dE'_e$  is the differential cross section and  $R(E_e, E'_e)$  is the energy resolution function, which can be described by a gaussian form:

$$R(E_e, E'_e) = \frac{1}{\Delta\sqrt{2\pi}} \exp\left[-\frac{(E_e - E'_e)^2}{2\Delta^2}\right]. \quad (49)$$

The energy resolution  $\Delta$  and the other parameters of the detectors (volume, efficiency, etc.) are summarized in the Appendix A.

The energy spectrum (48) of the charged leptons reflects the spectrum of the neutrinos, with the following differences:

- the energy dependence of the cross section<sup>2</sup>,  $\sigma \propto E^2$ , substantially enhances the high energy part of the spectrum.
- the integration over the neutrino energy and the convolution with the energy resolution function, eq. (48), lead to averaging out the fast modulations in low energy part of the spectrum (appearing for LMA oscillation parameters). Conversely, the large-period oscillations at high energies will appear in the lepton spectrum (48).

## 6.2 Identification of the Earth matter effects

The Earth matter effects can be identified:

1. at a single detector, by the observation of deviations of the energy spectrum with respect to what expected from conversion in the star only.
2. by the comparison of energy spectra from different detectors.

In the figs. 16-19 we show examples of the spectra expected at SK, SNO and LVD for oscillation parameters from the LMA solution,  $P_H = 1$  and various arrival times of the neutrino burst. We considered a supernova located in the direction of the galactic center (fig. 1 a)) at a distance  $D = 10$  Kpc and releasing a total energy  $E_B = 3 \cdot 10^{53}$  ergs. The histograms represent the numbers of events from the reaction (41) for SK (panels a)) and LVD (panels b)); the panels c) show the sum of the numbers of events from the reactions (43) and (41) at SNO. In d) we plot the numbers of events in the inner volume of SNO from the scattering (42).

As can be seen in fig. 1 a), for  $t = 1$  hour the neutrinos arriving at SK have core crossing trajectory ( $\cos \theta_n = 0.93$ ). For SNO the trajectory crosses the mantle only and is rather superficial ( $\cos \theta_n = 0.10$ ); the LVD detector is not shielded by the Earth. The

---

<sup>2</sup>The  $\sigma \propto E^2$  dependence constitutes a good approximation at low energies; in the highest energy part of the supernova neutrino spectrum deviations due to weak magnetism and recoil effects are relevant, see e.g. [37, 38, 39]. In our calculations we used the cross sections in ref. [39] for the scattering (41) and in ref. [40] for the reactions (42)-(43).

corresponding spectra are shown in fig. 16 for  $\Delta m_{\odot}^2 = 5 \cdot 10^{-5} \text{ eV}^2$  and  $\sin^2 2\theta_{\odot} = 0.75$  and the same temperatures as in the figs. 4 and 9 (see section 2.1). The spectrum of SK events exhibits deviations from the undistorted spectrum in some isolated bins, which correspond to the minima in the antineutrino spectrum. At SNO the Earth effect produces a narrowing of the spectrum. The difference with respect to the SK spectrum is attributed to the smaller oscillation phase (shorter trajectory in the Earth) of the neutrinos arriving at SNO.

The comparison of the results of the three experiments can be performed in various ways. If the direction to the supernova is determined, the LVD spectrum is known to be free from regeneration effects. Therefore it can be used to predict the energy distributions at SK and SNO without Earth matter effects. Such predictions can be compared to the observations of SNO and SK. Due to the relatively small statistics of the LVD events, however, the accuracy of the reconstruction will not be high and the deviation from the undistorted spectrum (e.g. in the range 40 - 65 MeV) will not be larger than  $2\sigma$ .

Higher statistical significance is obtained if data from a second large volume detector are available. Kilometer-scale neutrino telescopes, though primarily devoted to the study of high-energy neutrinos, are expected to be sensitive to supernova neutrinos. In particular, for a supernova at distance  $D = 10 \text{ Kpc}$  the ice Cerenkov detector of AMANDA [41] would observe more than  $2 \cdot 10^4$  events from  $\bar{\nu}_e$  scattering on protons, eq. (41) [42, 43]. Unfortunately, the presence of a relatively large background and the absence of sensitivity to the neutrino energy spectrum [42, 43, 44] strongly restrict the potential of the study of this signal. We mark, however, that substantial upgrades of the experimental apparatus are possible [44] and the optimization of the detector for supernova neutrino observation would be of great interest. Besides the present neutrino telescopes, the detection of supernova neutrinos is among the goals of future large volume detectors, like UNO [45] and NUSL [46]. We find that the comparison of the energy spectra observed by SK and by another detector with comparable or larger statistics could establish the Earth matter effects at more than  $\sim 5 \sigma$  level.

Even larger regeneration effect can be realized due to specific features of the original neutrino spectra and of the solution of the solar neutrino problem. The figure 17 shows the same spectra as fig. 16 for  $\Delta m_{\odot}^2 = 3 \cdot 10^{-5} \text{ eV}^2$ ,  $\sin^2 2\theta_{\odot} = 0.9$ ,  $T_e = 3 \text{ MeV}$  and  $T_{\bar{e}} = 4 \text{ MeV}$ . In this case the regeneration effect is substantially larger (see also figs. 5 and 6) and can be established by SK-LVD comparison with high ( $\gtrsim 3 \sigma$ ) statistical significance. Notice also that the statistics of each experiment, and therefore the power of the comparison between different detectors, is higher for smaller distance  $D$  to the supernova and/or larger binding energy  $E_B$ . For instance for  $D = 3 \text{ Kpc}$  and  $E_B \simeq 4.5 \cdot 10^{53} \text{ ergs}$  the statistics is  $\sim 17$  times higher and the differences between the spectra of SK and LVD (unshielded) can be as large as  $(6 - 10) \sigma$ .

Besides the comparison of the spectra, more specific criteria of identification of the Earth effect can be elaborated if the location of the supernova and the solar neutrino oscillations parameters are known. For instance, for LMA parameters and rather superficial trajectory in the mantle the effect consists in a narrowing of the spectrum (see e.g. figs. 16-17

panels c)-d)). Thus the comparison of the widths of the spectra at different detectors may establish the Earth effect.

As a further illustration, in figs. 18 and 19 we show the expected spectra for the same parameters as in fig. 16 but different arrival times of the signal (see fig. 1 a)). For  $t = 8$  hours SNO is unshielded while SK and SNO have deep trajectories in the mantle. For  $t = 17$  hours SNO has core crossing trajectory ( $\cos \theta_n \simeq 1$ ) and LVD observes effects of regeneration in the mantle only; SK is unshielded.

For neutrino parameters from the SMA solution the Earth effects on the spectra are smaller than  $\sim 5 - 10\%$ . This is explained by the fact that the narrow resonance peaks appear in the low energy part of the spectrum where the smoothing effect of the integrations (48) is stronger, thus suppressing the effect. Moreover, in the low energy region the detection cross sections and efficiencies are small. Therefore, regeneration effects with SMA parameters appear difficult to be observed. Similar conclusions hold for the case of LOW parameters, for which the effect is small and localized at low energies.

As we have mentioned in sect. 3.4, already the very fact of establishing the Earth matter effect in the neutrino and/or in antineutrino channel will have important implications for the neutrino mass and flavor spectrum. For this it will be enough to study some integral effect of regeneration. Let us consider the following possibility. As we have discussed in sect. 4, for LMA parameters the regeneration effect is negative above the critical energy and moreover the relative size of the effect increases with  $E$ . The Earth matter effect at low energy is small mainly due to the dependence of the regeneration factor  $f_{reg} \propto E$  (eq. (35)). Therefore to identify the regeneration effect one can compare the signals from the process (41) in the various detectors at low,  $E < E_s$ , and high,  $E > E_s$ , energies [47], where  $E_s$  is some separation energy. Let us introduce the numbers of events

$$N_L \equiv \int_{E_{th}}^{E_s} dE_e \frac{dN(\bar{\nu}p)}{dE_e}, \quad N_H \equiv \int_{E_s}^{\infty} dE_e \frac{dN(\bar{\nu}p)}{dE_e} \quad (50)$$

and the ratio

$$\mathcal{R} \equiv \frac{N_L}{N_H}. \quad (51)$$

In absence of Earth effects  $\mathcal{R}$  has the same value for every experiment provided that the detection efficiencies are independent of energy at  $E > E_{th}$ , or in the particular case of equal efficiencies. Therefore, differences in the quantity (51) are entirely due to regeneration effects: stronger effect corresponds to larger  $\mathcal{R}$ . In fig. 20 we show the dependence of  $\mathcal{R}$  on the separation energy  $E_s$  for different detectors; we have taken  $E_{th} = 20$  MeV. The panels a) and b) of the figures refer to the situations illustrated in figs. 16 and 17 respectively. In agreement with the analyses of the spectra, in the latter case (panel b)) the effect is stronger: the deviation of the ratio  $\mathcal{R}$  for SK from the value  $\mathcal{R}_0$  in absence of regeneration, given by LVD, can be as large as  $(2 - 3) \sigma$ . Larger deviation  $((4 - 5) \sigma)$  is realized if  $\mathcal{R}_0$  is provided by an experiment with volume comparable or larger than the one of SK.

## 7 Discussion

Within 2 - 3 years the solution of the solar neutrino problem can be identified by the results of the SNO, KamLAND and BOREXINO experiments. In particular, KamLAND will be able to establish the LMA solution and to measure  $\Delta m_{\odot}^2$  and  $\sin^2 2\theta_{\odot}$  with 10 - 20% accuracy [48, 49, 50, 51]. This will enormously sharpen the predictions for the Earth matter effects.

The possibility exists that  $U_{e3}$  will be determined by MINOS [52] provided that its value is not too far from the present upper bound, eq. (7). In this case,  $U_{e3}$  is certainly in the adiabatic range. In a long perspective, a neutrino factory [53] will be able to cover the whole the range of  $U_{e3}$  relevant for supernova neutrinos. Thus, either  $U_{e3}$  will be measured or the upper bound on  $U_{e3}$  will be so strong that the transition in the supernova will be certainly non-adiabatic.

Let us consider possible implications of the supernova neutrino results depending on the solution of the solar neutrino problem.

1). Suppose that the LMA solution will be identified with parameters close to the present best fit point ( $\Delta m_{\odot}^2 = (3 - 6) \cdot 10^{-5} \text{ eV}^2$ ). As we have seen, in this case the regeneration effect can be observed.

The features of the Earth matter effects depend on the value of  $U_{e3}$  and on the type of mass hierarchy. For normal mass hierarchy and  $U_{e3}$  in the adiabatic range (which appears as the most plausible scenario) we expect regeneration effects in the antineutrino channel and no effect in the neutrino channel (see sect. 3.4). In the supernova data further confirmations of such a possibility are (i) the absence of the neutronization peak in  $\nu_e$  and appearance of the  $\nu_{\mu}/\nu_{\tau}$  neutronization peak, (ii) hard spectrum of  $\nu_e$  during the cooling stage:  $\langle E_e \rangle > \langle E_{\bar{e}} \rangle$ .

The relative size of the effect in  $\bar{\nu}_e$  channel,  $\bar{R}$ , is determined by the regeneration factor and the flux factor, according to eq. (14). At high energies, when the flux factor reaches the asymptotic value (17), eq. (14) gives:

$$\bar{R}(E \gg \bar{E}_c) \sim -\frac{\bar{f}_{reg}}{\sin^2 \theta_{\odot}}. \quad (52)$$

That is, the effect is completely predicted in terms of solar oscillation parameters.

In the case of inverted mass hierarchy the Earth matter effect should be observed in the neutrino channel and no effect is expected in the antineutrino channel if  $|U_{e3}|^2 > 10^{-5}$  (see fig. 2). This possibility will be confirmed by the observation of the  $\nu_e$ -neutronization peak and of an hard spectrum of the  $\bar{\nu}_e$  during the cooling stage. The relative size of the Earth matter effect,  $R$ , is given by eq. (37) (with the replacement  $P_H \rightarrow 1$ ) with the high energy asymptotic (see eq. (40))

$$R(E \gg E_c) \sim -\frac{f_{reg}}{\cos^2 \theta_{\odot}}. \quad (53)$$

In the limit  $|U_{e3}|^2 \ll 10^{-5}$  the high density resonance is inoperative, so that the result is insensitive to the mass hierarchy. Oscillations appear in both the neutrino and antineutrino channels, and, at high energies, they are determined by the solar oscillation parameters (eqs. (52) and (53)). The ratio of the relative effects at high energies equals:

$$\frac{R}{\bar{R}} \simeq \tan^2 \theta_{\odot} \frac{f_{reg}}{\bar{f}_{reg}}. \quad (54)$$

So, possible checks of this equality would be the confirmation of the neutrino scheme with very small  $U_{e3}$ .

If  $U_{e3}$  is in the intermediate region:  $|U_{e3}|^2 \sim 10^{-6} - 10^{-5}$  the situation is more complicated. One expects to observe oscillations both in the neutrino and antineutrino channels; the regeneration effect depends on the mass hierarchy and on the specific value of  $U_{e3}$ . In the case of normal mass hierarchy, the relative effect in the neutrino channel is proportional to  $P_H = P_H(U_{e3})$  (eq. (37)) and at high energies, when the flux factor reaches the asymptotic value we get, (eq. (40)):

$$R(E \gg E_c) \sim -\frac{P_H}{1 - P_H \sin^2 \theta_{\odot}} f_{reg}. \quad (55)$$

Since  $f_{reg}$  is determined by the solar parameters, by measuring the relative deviation  $R$  we can determine the value of  $P_H$  via the eq. (55) and therefore get information about  $U_{e3}$ .

For antineutrinos with inverted hierarchy we find the high energy asymptotic (see eq. (36)):

$$\bar{R}(E \gg \bar{E}_c) \sim -\frac{P_H}{1 - P_H \cos^2 \theta_{\odot}} \bar{f}_{reg}. \quad (56)$$

In practice, the observation of the Earth matter effect in the  $\bar{\nu}_e$  channel and absence of the effect in  $\nu_e$  channel will testify for normal mass hierarchy and  $|U_{e3}|^2 > 10^{-5}$ . In the opposite situation, effect in the  $\nu_e$  channel and absence of the effect in  $\bar{\nu}_e$  channel, the inverted hierarchy will be identified with  $|U_{e3}|^2 > 10^{-5}$ . However the present experiments have lower sensitivity to  $\nu_e$  fluxes with respect to the fluxes of  $\bar{\nu}_e$ , so that it may be difficult to establish “zero” regeneration effect with high enough accuracy.

If the Earth matter effect is observed in both channels, one should compare the size of the effect with that predicted in the absence of the high resonance in a given channel. Thus, if the observed signal in the neutrino channel is smaller than what is predicted in the assumption of  $P_H = 1$ , whereas in the antineutrino channel prediction and observation coincide, we will conclude that the hierarchy is normal and the ratio of the observed to predicted signals in the neutrino channel can give the value of  $P_H$ . The opposite case of

coincidence of the predicted and observed signals in the neutrino channel and suppressed observed signal in the antineutrino channel will testify for the inverted mass hierarchy.

Besides the probing of the neutrino mass spectrum and mixing, a study of the properties of the original neutrino fluxes can be done with Earth matter effects. In principle, a detailed study of the observed energy spectra will allow to reconstruct the flux factor as well as to determine the critical energy  $E_c$ .

2). Suppose that the future solar neutrino experiments will identify the SMA solution. In this case, the Earth matter effect is expected in the neutrino channel only, and only if the high density resonance is inoperative. This requires the inverted mass hierarchy or very small  $U_{e3}$  in the case of normal mass hierarchy. As discussed in sect. 5.2, the effect is small and difficult to be observed even in the most favorable situations.

For the rather plausible case of the normal mass hierarchy and  $|U_{e3}|^2 > 10^{-5}$  no Earth matter effect should be seen.

The observation of the Earth matter effect in the SMA case will allow to conclude that the mass hierarchy is inverted or the hierarchy is normal but  $U_{e3}$  is very small:  $|U_{e3}|^2 \ll 10^{-5}$ . In principle, the intermediate case  $|U_{e3}|^2 \sim 10^{-5}$  can be identified if the observed signal will be smaller than the expected one for  $P_H = 1$ . Notice that from eqs. (21) and (22) one gets the low energy asymptotic for the flux factor:

$$R(E \ll E_c) = P_H(1 - 2P_L)f_{reg}\frac{1}{P_HP_L} = f_{reg}(1 - 2P_L)\frac{1}{P_L}, \quad (57)$$

which does not depend on  $P_H$ . So it will be difficult to disentangle the effect of  $P_H$  from uncertainties in the original neutrino fluxes.

The situation can be much more complicated if a sterile neutrino exists. This can be clarified in 2 - 3 years: the MiniBooNE experiment and further searches for sterile neutrinos in the solar and atmospheric neutrino experiments will allow to establish the existence of sterile neutrinos.

Negative results of the searches will strongly favor the  $3\nu$  schemes discussed in this paper. Still some uncertainty will remain: sterile neutrinos, unrelated to the LSND result, may exist and weakly mix with active neutrinos. Even a very small mixing (unobservable by other means) of sterile states with masses in the wide range from sub eV up to 10 keV can strongly modify the properties of the neutrino burst.

## 8 Conclusions

1). There is a big chance that at least one of the existing detectors (SK, SNO, LVD) will be shielded by the Earth at the moment of arrival of a supernova neutrino burst, so that the Earth matter effect on the neutrino flux will be observed. For supernova in a region close to the galactic center the most plausible configuration is that for two detectors the trajectories of the neutrino burst cross the Earth, whereas the third detector is unshielded.



We found that the detectors considered can register Earth matter effects ( $\cos\theta_n > 0$ ) for a significant fraction ( $\gtrsim 60\%$ ) of the possible arrival times of the signal and core effect for  $\sim 20\%$  of the times. These fractions may be even larger depending on the specific location of the star in the galaxy.

The comparison of the signals from different detectors allows to identify the Earth matter effect and to get information on the neutrino mass spectrum, substantially reducing the uncertainties related to the model of the star and to the original neutrino fluxes.

2). We studied the effects of the matter of the Earth on supernova neutrinos in the framework of three flavours with either normal or inverted hierarchy.

3). The strongest regeneration effect is expected for oscillation parameters in the region of the LMA solution of the solar neutrino problem, especially for the lowest values of  $\Delta m_\odot^2$  in this region:  $\Delta m_\odot^2 = (2 - 5) \cdot 10^{-5} \text{ eV}^2$ .

In the  $\bar{\nu}_e$  – channel the effect exists in the scheme with normal mass hierarchy (ordering of the states) or in the scheme with inverted mass hierarchy for  $|U_{e3}|^2 < 10^{-5}$ , when the conversion in the high density resonance is non-adiabatic. The effect consists in an oscillatory modulation of the energy spectra and is negative (except in small energy intervals for core crossing trajectories) above the critical energy  $E_c \sim 25 \text{ MeV}$ , thus suppressing the signal. The relative size of the effect increases with energy and at  $E \sim 60 - 70 \text{ MeV}$  it can reach  $50 - 70\%$ . The period of modulation increases with energy and above  $E \sim 40 \text{ MeV}$  no averaging occurs in the energy spectrum of events. At low energies the effect is small and the modulations are averaged out. Thus, in the LMA case the most sensitive region to the Earth matter effect is above  $E \sim 40 \text{ MeV}$ .

The oscillatory picture (position of minima and maxima) is very sensitive to  $\Delta m_\odot^2$ . For trajectories in the mantle only the modulation of the spectrum is rather regular. For the core-crossing trajectories the structures become narrower and irregular.

The Earth matter effect decreases with the increase of  $\Delta m_\odot^2$  and for  $\Delta m_\odot^2 > 10^{-4} \text{ eV}^2$  it will be difficult to be observed.

4). For the  $\nu_e$  – channel substantial Earth matter effect is expected in the case of normal mass hierarchy, provided that  $|U_{e3}|^2 < 10^{-5}$ , or in the case of inverted mass hierarchy. The effect has oscillatory character, similarly to the  $\bar{\nu}_e$  – case, and can be as large as  $100\%$  at  $E > 50 - 60 \text{ MeV}$ .

Thus, as in the case of antineutrinos, one should search for an oscillatory modulation of the signal in the energy range  $E > 40 \text{ MeV}$ .

The size of the effect depends on the properties of the original neutrino fluxes via the flux factor. This dependence, however, disappears in the high-energy limit,  $E \gtrsim 50 \text{ MeV}$ .

5). For oscillation parameters from the SMA solution the effect appears in the  $\nu_e$  – channel only, and only if the H-resonance is inoperative (very small  $U_{e3}$  or inverted mass hierarchy). The relative effect can be as large as  $30\%$  for core crossing trajectories due to the parametric enhancement of oscillations. The effect is localized in the low energy

part of the spectrum:  $E = 5 - 10$  MeV. It can be further suppressed by the L-resonance factor  $(1 - 2P_L)$  which in turn strongly depends on the density profile of the star in the outer region. The effect will be strongly smoothed in the spectrum of observed events by integrations over the neutrino energy and the true energy of electron. Practically no distortion is seen and the effect is reduced to an increase of the number of events in the region of the peak. Effectively this will make the spectrum narrower. One can probably identify this effect by comparing the signals from two high statistics experiments.

6). In the case of LOW solution the Earth matter effect is significant at very low energies with a smooth  $1/E$  behaviour. If the H-resonance is inoperative, in the  $\nu_e$  channel the effect (excess of flux) can reach 100% at  $E = 1$  MeV and 20% in the  $\bar{\nu}_e$  channel (the difference is mainly due to the difference in the flux factors). At  $E = 5$  MeV, the effect in the flux is below  $(10 - 20)\%$ . The nadir angle dependence is determined by the length of the trajectory: the oscillation length almost equals the refraction length and depends only weakly on the neutrino energy. For the core crossing trajectories the effects can be enhanced due to parametric effects.

7). The identification of the Earth matter effect is possible in a single detector (in the LMA case) by the observation of the oscillatory modulation of the energy spectrum in the high energy part:  $E > 40$  MeV. Another method consists in the comparison of signals from two (or several) different detectors. If one of the detectors is unshielded by the Earth its result can be used to reconstruct the spectrum of the neutrinos arriving at Earth and make predictions of the signal expected in the other detectors in absence of matter effect. For a supernova at distance  $D = 10$  Kpc and with energy release  $E_B = 3 \cdot 10^{53}$  ergs we estimated that the Earth matter effects can be established at  $(2 - 3)\sigma$  level by comparison between SK, SNO and LVD results, and at  $(4 - 5)\sigma$  by comparison between the spectra from two large volume detectors (of SK size or larger).

Another method to identify the Earth matter effect is to study the ratio of numbers of events in the high and in the low parts of the spectrum in different detectors.

8). Studies of the Earth matter effect will allow to establish or most probably to confirm the solution of the solar neutrino problem, to get information about  $U_{e3}$  and to identify the type of hierarchy of the neutrino mass spectrum.

## Acknowledgements

The authors are grateful to P. Antonioli and W. Fulgione for discussions and for providing material on the LVD experiment. Thanks also to H. Robertson for giving information on the SNO detector and to J. Beacom for helpful comments. C.L. wishes to thank A. Friedland, P. Krastev, C. Burgess, A. Bouchta, C. De Los Heros and R. Hubbard for useful discussions.

## Appendix A. Parameters of detectors

We summarize here the characteristics of the SK, SNO and LVD detectors that have been used in the analysis of section 6.2.

For each experiment we consider:

1. The position of the detector on the Earth, which is relevant for determining the trajectory of the observed neutrinos inside the Earth (see sect. 2.2). The locations of the three experiments are given in Table 1 in terms of northern latitude,  $\delta$ , and eastern longitude  $\alpha$ .
2. The material which the detector is made of and its fiducial mass. These quantities are quoted in Table 1.
3. The detection efficiency  $\mathcal{E}(E'_e)$  (see eq. (48)).

The SNO efficiency is high, so that the shape of the energy spectrum and the total number of events are determined by the detection cross section [54]. Therefore, we have taken  $\mathcal{E} = 1$  in eq. (48).

The efficiency of the LVD detector has been provided by the dedicated collaboration [55]. For  $E_{th} \leq 10$  MeV, it is given by the gaussian integral function:

$$\mathcal{E}(E_m, E_{th}) = \frac{1}{\sqrt{2\pi}} \int_{-\infty}^x e^{-\frac{y^2}{2}} dy , \quad (58)$$

where  $x \equiv (E_m - E_{th})/\sigma_{th}$  and  $E_m$  is the measured energy of the lepton. The values of the parameters  $E_{th}$  and  $\sigma_{th}$  are:  $E_{th} = 4$  MeV and  $\sigma_{th} = 0.74$  MeV for the core counters (mass  $M = 0.57$  ktons);  $E_{th} = 7$  MeV and  $\sigma_{th} = 1.1$  MeV for the external counters (mass  $M = 0.43$  ktons).

For SK we adopted the efficiency published for the Kamiokande-2 experiment [56].

4. The energy resolution  $\Delta$ , which appears in the resolution function (49). We followed ref. [57] for SK and SNO experiments, and refs. [58, 55] for LVD. The parameter  $\Delta$  depends on energy as follows:

$$\frac{\Delta}{\text{MeV}} = A \frac{E_e}{\text{MeV}} + B \sqrt{\frac{E_e}{\text{MeV}}} . \quad (59)$$

The values of the coefficients  $A$  and  $B$  are given in Table 1.

## Appendix B. The regeneration factor: step-like and realistic Earth profile

The analytical expressions for the regeneration factors (23) and (13) can be obtained in the two layers approximation of the Earth density profile. In this approximation the mantle and the core of the Earth are considered as layers with constant densities. Therefore

detector	$\delta$	$\alpha$	material	mass (ktons)	A	B
SK	36°21'	137°18'	H <sub>2</sub> O	32	0	0.5
SNO	46°30'	−81°01'	H <sub>2</sub> O	1.4	0	0.35
			D <sub>2</sub> O	1.0		
LVD	42°25'	13°31'	(CH <sub>2</sub> ) <sub>10</sub>	1.0	0.07	0.23

Table 1: Summary of the characteristics of the detectors we consider, in particular their locations on the Earth (in terms of northern latitude  $\delta$  and eastern longitude  $\alpha$ ), the fiducial masses and the coefficients  $A$  and  $B$  which appear in the expression of the energy resolution, eq. (59).

the neutrinos experience a constant matter potential along trajectories in the mantle and a step-like profile mantle-core-mantle along core crossing trajectories. In what follows we summarize the analytical results obtained in the two-layers approximation, which correctly describe the general features of the Earth matter effects. The comparison with exact numerical calculations will be given at the end of this appendix.

For  $\nu_e$  propagating in the mantle only the regeneration factor,  $f_{reg}$ , eq. (23), has the form:

$$f_{reg} = D(E, \theta, \theta_n, \rho_m) \sin^2 \left( \pi \frac{d}{l_m} \right) , \quad (60)$$

where  $d = 2R_{\oplus} \cos \theta_n$  is the length of the trajectory in the Earth,  $R_{\oplus} \simeq 6400$  Km is the radius of the Earth and  $\rho_m$  the matter density in the mantle. The depth  $D$  of oscillations equals [13]:

$$D = \sin 2\theta_m \sin(2\theta_m - 2\theta) , \quad (61)$$

with  $\theta_m$  and  $l_m$  being the mixing angle and the oscillation length in matter and  $\theta$  the mixing angle in vacuum.

Since the mixing is enhanced in matter,  $\theta_m > \theta$ , the depth  $D$  is positive as well as the whole regeneration factor (60). From eq. (61) one gets:

$$D = x \frac{\sin^2 2\theta}{(x - \cos 2\theta)^2 + \sin^2 2\theta} , \quad (62)$$

where

$$x = \frac{2EV}{\Delta m^2}$$

and  $V$  is the matter potential. The expression (62) vanishes in the limits of low ( $x \ll 1$ ) and high ( $x \gg 1$ ) energies. It reaches the maximum

$$D_{max} = \cos^2 \theta , \quad (63)$$

at  $x = 1$ , which corresponds to the energy:

$$E_R = \frac{\Delta m^2}{2\sqrt{2}G_F n_e} . \quad (64)$$

Here  $G_F$  is the Fermi constant and  $n_e$  the electron number density in the medium.

Thus, the depth of oscillations,  $D$ , has a resonant character with  $E = E_R$  being the resonance condition. The width of the resonance is given by the interval  $E_- \div E_+$  in which  $D \geq D_{max}/2$ . One finds:

$$\frac{E_{\pm}}{E_R} = 2 - \cos 2\theta \pm \sqrt{(1 - \cos 2\theta)(3 - \cos 2\theta)} , \quad (65)$$

which shows that the peak at  $E \sim E_R$  is wide for LMA oscillation parameters and gets narrower as  $\theta$  decreases. Notice that in the limit  $\theta \rightarrow 0$  the maximal depth increases,  $D_{max} \rightarrow 1$ , but the oscillations disappear due to the decrease of the oscillation phase and the vanishing of the resonance width (see eq. (65)).

For antineutrinos, and trajectory in the mantle only, the regeneration factor  $\bar{f}_{reg}$ , eq. (13), has the same form as in eq. (60), with the oscillation depth

$$\begin{aligned} \bar{D} &= -\sin 2\theta_m \sin(2\theta_m - 2\theta) , \\ &= x \frac{\sin^2 2\theta}{(x + \cos 2\theta)^2 + \sin^2 2\theta} , \end{aligned} \quad (66)$$

where we defined

$$x \equiv \frac{2E|V|}{\Delta m^2} .$$

Similarly to the case of  $\nu_e$  the depth  $\bar{D}$ , and therefore the regeneration factor  $\bar{f}_{reg}$ , is positive, since  $\theta_m < \theta$ ; moreover it has a similar resonant behaviour with maximum

$$\bar{D}_{max} = \sin^2 \theta , \quad (67)$$

and the same resonance energy, eq. (64). The borders  $E_-, E_+$  of the resonance interval are given by eq. (65) with the replacement  $\cos 2\theta \rightarrow -\cos 2\theta$ . In the limit  $\theta \rightarrow 0$  the Earth effect disappears due to the vanishing of the oscillation depth (67). For maximal mixing,  $\cos 2\theta = 0$ , we get

$$D = \bar{D} = \frac{x}{x^2 + 1} .$$

If the neutrino trajectory crosses both the mantle and the core the analytical treatment of the regeneration factors,  $\bar{f}_{reg}$  and  $f_{reg}$ , is more complicated [59]. The interplay of oscillations in the mantle and in the core determine irregular oscillations of the factors with energy. The depth of oscillations is larger in the region of the energy spectrum close to the resonance energies in the mantle and in the core; for SMA oscillation parameters parametric effects appear (see fig. 15). In contrast to the propagation in the mantle only (i.e. in uniform medium), the regeneration factors have negative sign in some intervals of energy.

Once a realistic density profile of the Earth is considered, the calculation of the regeneration factors requires a numerical treatment. The results are presented in fig. 21 together with the analytical curves obtained with the two-layers approximation. The figure shows the factors  $\bar{f}_{reg}$  and  $f_{reg}$  as functions of the neutrino (antineutrino) energy for  $\Delta m^2 = 5 \cdot 10^{-5} \text{ eV}^2$ ,  $\sin^2 2\theta = 0.75$  and  $\theta_n = 0^\circ$ . We used the realistic profile in ref. [35] and chose a step-like (two-layers) profile with densities  $\rho_m = 4.51$  and  $\rho_c = 11.95$ , corresponding to the average densities of the profile of ref. [35] in the mantle and in the core along the diameter of the Earth.

From the figure 21 it follows that the position of the oscillation maxima and minima on the energy axis are well reproduced by the step profile. This good approximation of the oscillation phase is ascribed to the choice of  $\rho_m$  and  $\rho_c$  to be the average densities of the two layers along the trajectory of the neutrinos.

In contrast, the depth of oscillations given by the numerical calculation deviates significantly, up to  $\sim 50\%$ , from the result of the analytical (two-layers) approximation. As a general tendency, the depth of oscillations in the realistic density profile appears smaller with respect to the case of the two-layers profile. If the density jumps along the trajectory are not very large (e.g. for trajectories in the mantle only) this feature can be interpreted, qualitatively, by considering the density as smoothly varying along the path of the neutrinos. In this case the neutrino conversion occurs adiabatically and the depth of oscillations is determined by the matter density at the surface of the Earth. Since the surface density is smaller than the average density along the trajectory and the latter in turn is smaller than the resonance density  $\rho_R$  in the relevant range of energies, a smaller depth of oscillations is expected.

A better approximation of the numerical results can be obtained by using the average density in the determination of the oscillation phase and the surface density in the determination of the depth of oscillations.

For SMA parameters the adiabaticity is broken and the two layers model gives a good approximation of the numerical results.

## References

- [1] S. P. Mikheev and A. Y. Smirnov, *Sov. Phys. JETP* 64 (1986) 4.
- [2] S.P. Mikheev and A.Y. Smirnov, *Proceedings of the 6th Moriond Workshop Massive Neutrinos in Astrophysics and in Particle Physics*, 1986, edited by O. Fackler and J. Tran Than Van (Editions Frontières, Gif-sur-Yvette, France, 1986), p. 355.
- [3] A. Y. Smirnov, talk given at the *Twentieth International Cosmic Ray Conference*, Moscow, 1987.
- [4] J. Arafune and M. Fukugita, *Phys. Rev. Lett.* 59 (1987) 367.
- [5] J. Arafune et al., *Phys. Rev. Lett.* 59 (1987) 1864.

- [6] H. Minakata et al., *Mod. Phys. Lett. A*2 (1987) 827.
- [7] P.O. Lagage et al., *Phys. Lett. B*193 (1987) 127.
- [8] D. Notzold, *Phys. Lett. B*196 (1987) 315.
- [9] S.P. Rosen, *Phys. Rev. D*37 (1988) 1682.
- [10] T.K. Kuo and J. Pantaleone, *Phys. Rev. D*37 (1988) 298.
- [11] H. Minakata and H. Nunokawa, *Phys. Rev. D*38 (1988) 3605.
- [12] L. Wolfenstein, *Phys. Lett. B*194 (1987) 197.
- [13] A. Y. Smirnov, D. N. Spergel and J. N. Bahcall, *Phys. Rev. D*49 (1994) 1389 [hep-ph/9305204].
- [14] A. S. Dighe and A. Y. Smirnov, *Phys. Rev. D*62 (2000) 033007 [hep-ph/9907423].
- [15] B. Jegerlehner, F. Neubig and G. Raffelt, *Phys. Rev. D*54 (1996) 1194 [astro-ph/9601111].
- [16] C. Lunardini and A.Y. Smirnov, *Phys. Rev. D*63 (2001) 073009 [hep-ph/0009356].
- [17] H. Minakata and H. Nunokawa, *Phys. Lett. B*504 (2001) 301 [hep-ph/0010240].
- [18] M. Kachelriess, R. Tomas and J.W.F. Valle, *JHEP* 01 (2001) 030 [hep-ph/0012134].
- [19] H. Minakata, *Nucl. Phys. Proc. Suppl.* 100 (2001) 237 [hep-ph/0101231].
- [20] K. Takahashi, M. Watanabe and K. Sato, (2000), hep-ph/0012354.
- [21] G. E. Brown, H. A. Bethe and G. Baym, , *Nucl. Phys. A* 375 (1982) 481.
- [22] H. T. Janka and W. Hillebrandt, *Astron. Astroph. Suppl.* 78 (1989) 375, *Astron. Astrophys.* 224 (1989) 49.
- [23] S.P. Mikheev and A.Y. Smirnov in ref. [2]; for a detailed discussion of regeneration of solar neutrinos see e.g. E. Lisi and D. Montanino, *Phys. Rev. D*56 (1997) 1792 [hep-ph/9702343].
- [24] For a review on supernova neutrino experiments see K. Scholberg, *Nucl. Phys. Proc. Suppl.* 91 (2000) 331 [hep-ex/0008044].
- [25] See W. Fulgione for the LVD collaboration, *Nucl. Phys. Proc. Suppl.* 70 (1999) 469, and references therein.
- [26] See C.J. Virtue for the SNO collaboration, *Nucl. Phys. Proc. Suppl.* 100 (2001) 326 [astro-ph/0103324], and references therein.

- [27] The Super-Kamiokande collaboration, Y. Fukuda et al., Phys. Rev. Lett. 81 (1998) 1158 [hep-ex/9805021].
- [28] See J.F. Beacom and P. Vogel, Phys. Rev. D60 (1999) 033007 [astro-ph/9811350], and references therein.
- [29] A study was presented by the CHOOZ collaboration, M. Apollonio et al., Phys. Rev. D61 (2000) 012001 [hep-ex/9906011].
- [30] The Super-Kamiokande collaboration, S. Fukuda et al., Phys. Rev. Lett. 85 (2000) 3999 [hep-ex/0009001].
- [31] The CHOOZ collaboration, M. Apollonio *et al.*, Phys. Lett. B466 (1999) 415 [hep-ex/9907037]; Phys. Lett. B420 (1998) 397 [hep-ex/9711002].
- [32] F. Boehm et al., Phys. Rev. D62 (2000) 072002 [hep-ex/0003022].
- [33] J.N. Bahcall, P.I. Krastev and A.Y. Smirnov, JHEP 05 (2001) 015 [hep-ph/0103179].
- [34] A discussion of adiabaticity in the context of supernova neutrinos is given in M. Kachelriess and R. Tomas, hep-ph/0104021; see also references therein.
- [35] A. M. Dziewonski and D. L. Anderson, Phys. Earth. Planet. Inter. 25 (1981) 297.
- [36] M.C. Gonzalez-Garcia, C. Pena-Garay and A.Y. Smirnov, Phys. Rev. D63 (2001) 113004 [hep-ph/0012313].
- [37] P. Vogel, Phys. Rev. D29 (1984) 1918.
- [38] S.A. Fayans, Sov. J. Nucl. Phys. 42 (1985) 590.
- [39] P. Vogel and J.F. Beacom, Phys. Rev. D60 (1999) 053003 [hep-ph/9903554]; see also J.F. Beacom and S.J. Parke, hep-ph/0106128.
- [40] S. Nakamura et al., Phys. Rev. C63 (2001) 034617 [nucl-th/0009012].
- [41] For review, see e.g. C. Spiering, Annalen Phys. 10 (2001) 131; G.C. Hill, (2001), astro-ph/0106064.
- [42] F. Halzen, J.E. Jacobsen and E. Zas, Phys. Rev. D53 (1996) 7359 [astro-ph/9512080].
- [43] The AMANDA collaboration, J. Ahrens et al., (2001), astro-ph/0105460.
- [44] A. Bouchta and C. De Los Heros for AMANDA collaboration, private communication.
- [45] C. K. Jung, hep-ex/0005046.
- [46] The recent NUSL proposal is available at <http://www.sns.ias.edu/~jnb/>.



- [47] A similar criterion was proposed in K. Takahashi et al., (2001), hep-ph/0105204.
- [48] V. Barger, D. Marfatia and B. P. Wood, Phys. Lett. B 498 (2001) 53 [hep-ph/0011251].
- [49] R. Barbieri and A. Strumia, JHEP 0012 (2000) 016 [hep-ph/0011307].
- [50] H. Murayama and A. Pierce, hep-ph/0012075.
- [51] For an experimental review see e.g. A. Piepke for the KamLAND collaboration, Nucl. Phys. Proc. Suppl. 91 (2001) 99.
- [52] S.G. Wojcicki, Nucl. Phys. Proc. Suppl. 91 (2001) 216.
- [53] A comprehensive review is given in C. Albright et al., (2000), hep-ex/0008064.
- [54] H. Robertson for SNO collaboration, private communication.
- [55] P. Antonioli and W. Fulgione for LVD collaboration, private communication.
- [56] K.S. Hirata et al., Phys. Rev. D38 (1988) 448.
- [57] J.N. Bahcall, P.I. Krastev and E. Lisi, Phys. Rev. C55 (1997) 494 [nucl-ex/9610010].
- [58] P. Antonioli et al., Nucl. Instrum. Meth. A309 (1991) 569.
- [59] See the review E.K. Akhmedov, Pramana 54 (2000) 47 [hep-ph/9907435], and references therein.

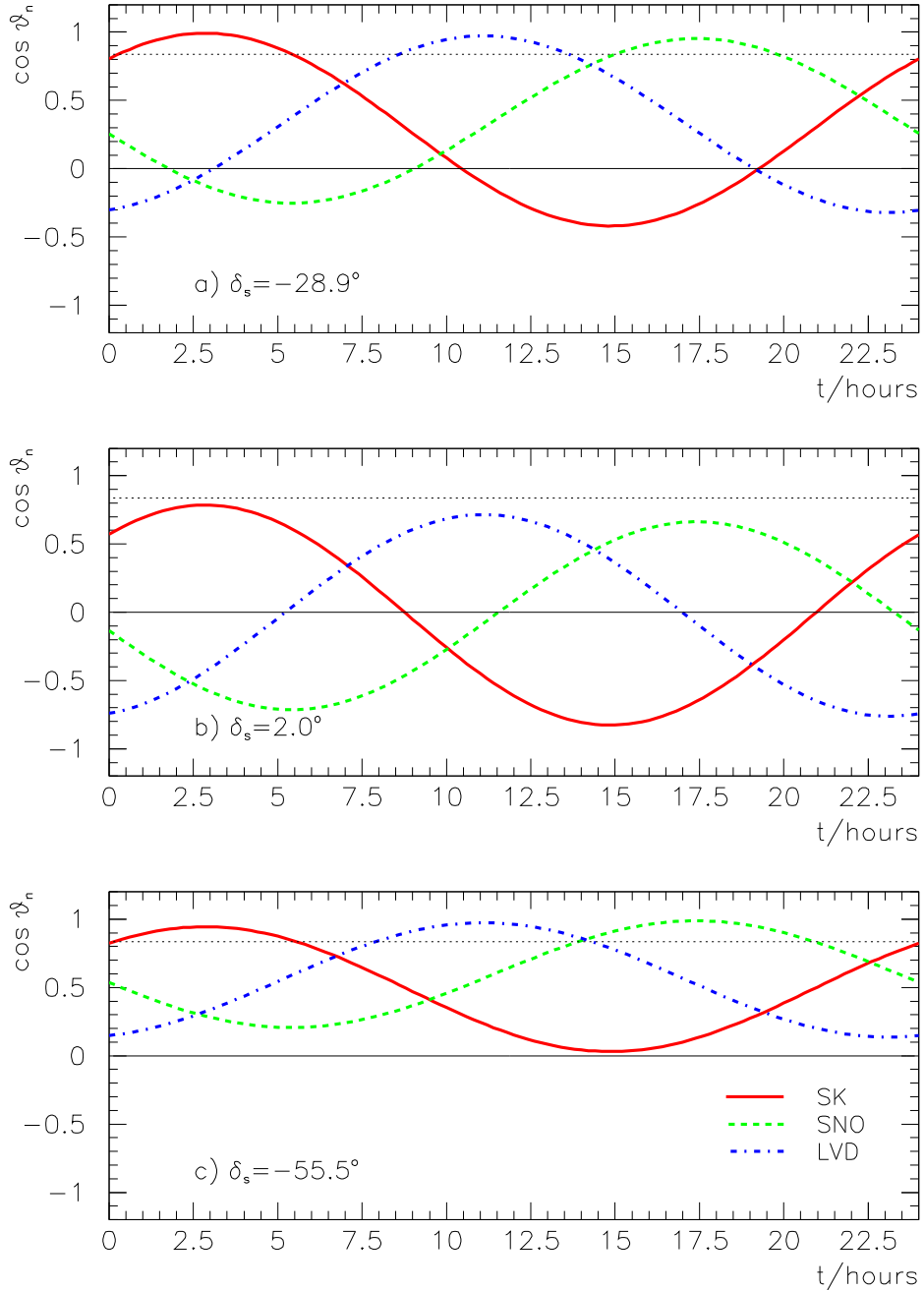


Figure 1: The cosines of the nadir angles  $\theta_n$  of SuperKamiokande, SNO and LVD detectors with respect to the supernova as functions of the arrival time of neutrino burst. The three panels refer to three different locations of the star in the galactic plane (given by the declination angle  $\delta_s$ ). We fixed  $t = 0$  as the time at which the star is aligned with the Greenwich meridian.

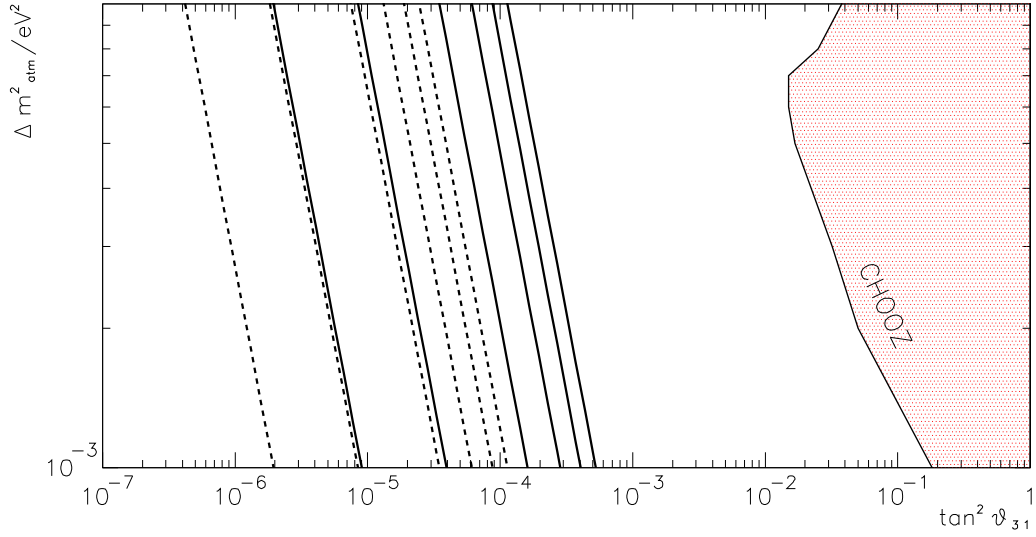


Figure 2: Lines of constant flip probability  $P_H$  in the  $\Delta m^2_{atm}$ - $\tan^2 \theta_{31}$  plane. The solid lines refer to  $E = 50$  MeV and correspond, from right to left, to  $P_H = 0.05, 0.1, 0.2, 0.4, 0.8, 0.95$ . The dashed lines correspond to the same values of  $P_H$  with  $E = 5$  MeV. The exclusion region from the CHOOZ experiment is shown.

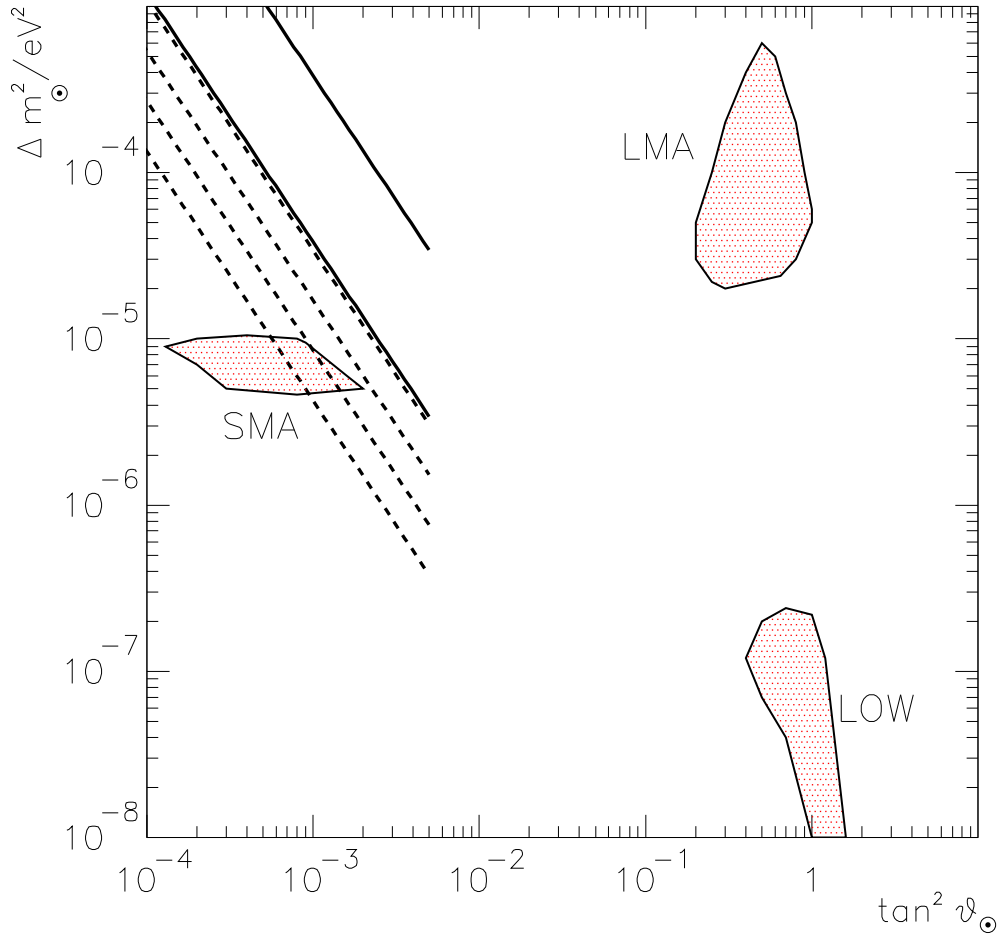


Figure 3: Lines of constant jump probability in the low density resonance,  $P_L$ , in the  $\tan^2 \theta_\odot$ - $\Delta m_\odot^2$  plane. The solid lines correspond to  $P_L = 0.05$ ,  $E = 50$  MeV (upper line) and  $E = 5$  MeV (lower line). The dashed lines correspond to  $P_L = 0.5$  and, from the upper to the lower,  $E = 40, 20, 10, 5$  MeV. The plot of the lines is restricted to the region of parameters for which the L-resonance inside the star occurs at densities larger than  $1 \text{ g} \cdot \text{cm}^{-3}$  (see sect. 2.1 of the text). The allowed regions for the SMA, LMA and LOW solutions of the solar neutrino problem are represented.

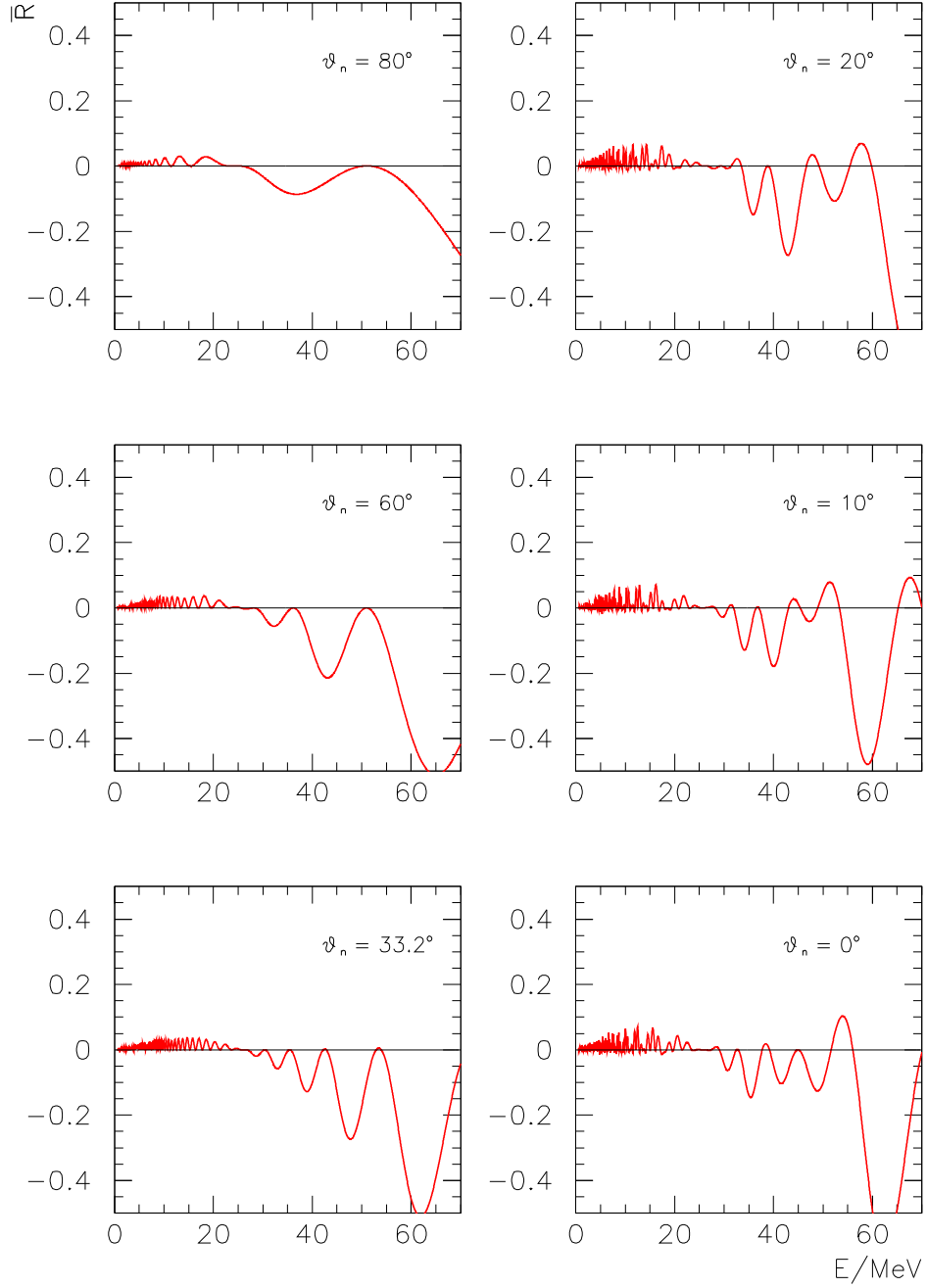


Figure 4: The relative Earth matter effect in  $\bar{\nu}_e$  channel,  $\bar{R}$ , as function of the antineutrino energy for LMA oscillation parameters and various values of the nadir angle  $\theta_n$ . We have taken  $\Delta m_{\odot}^2 = 5 \cdot 10^{-5} \text{ eV}^2$ ,  $\sin^2 2\theta_{\odot} = 0.75$ ;  $T_{\bar{e}} = 5 \text{ MeV}$ ,  $T_x = 8 \text{ MeV}$ . The figure refers to normal mass hierarchy (or inverted hierarchy with  $P_H = 1$ ).

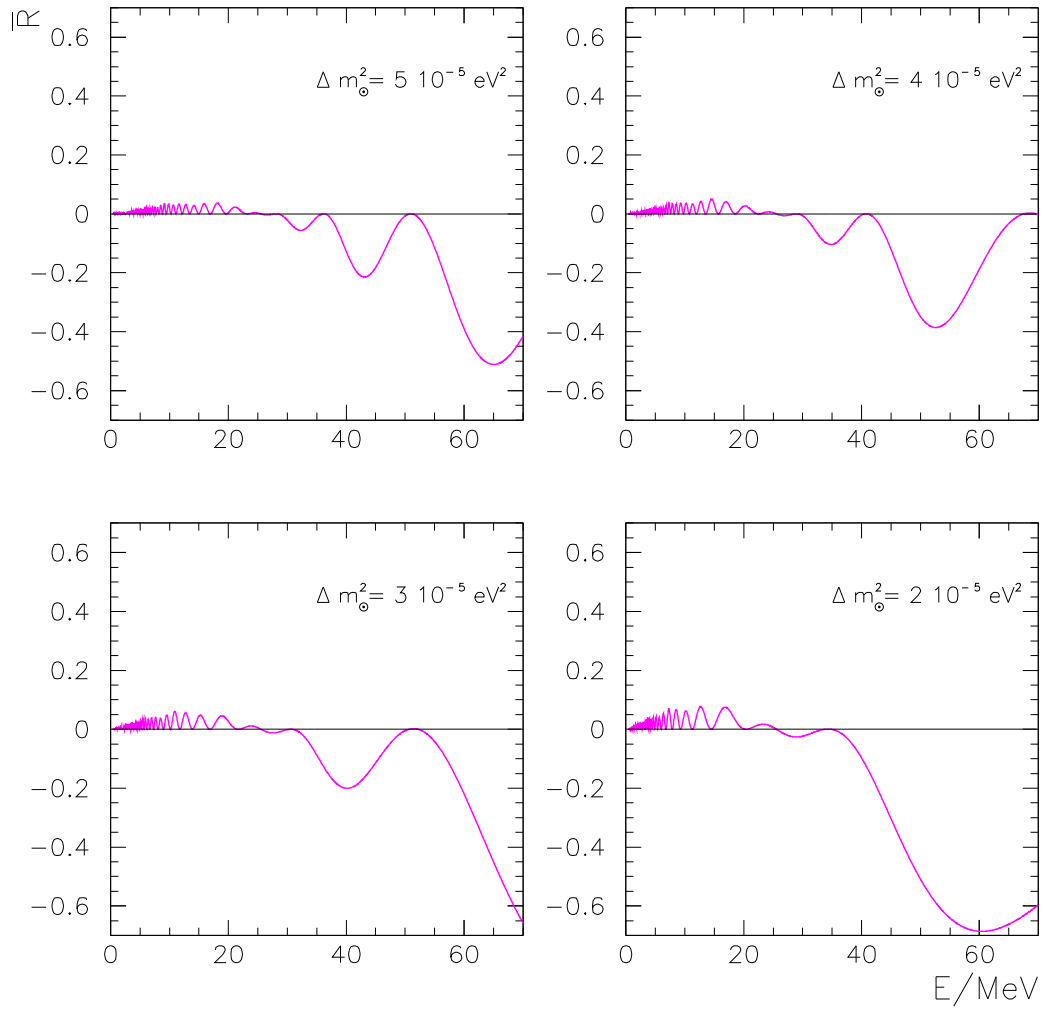


Figure 5: The same as fig. 4 for  $\theta_n = 60^\circ$  and various values of  $\Delta m_\odot^2$ .

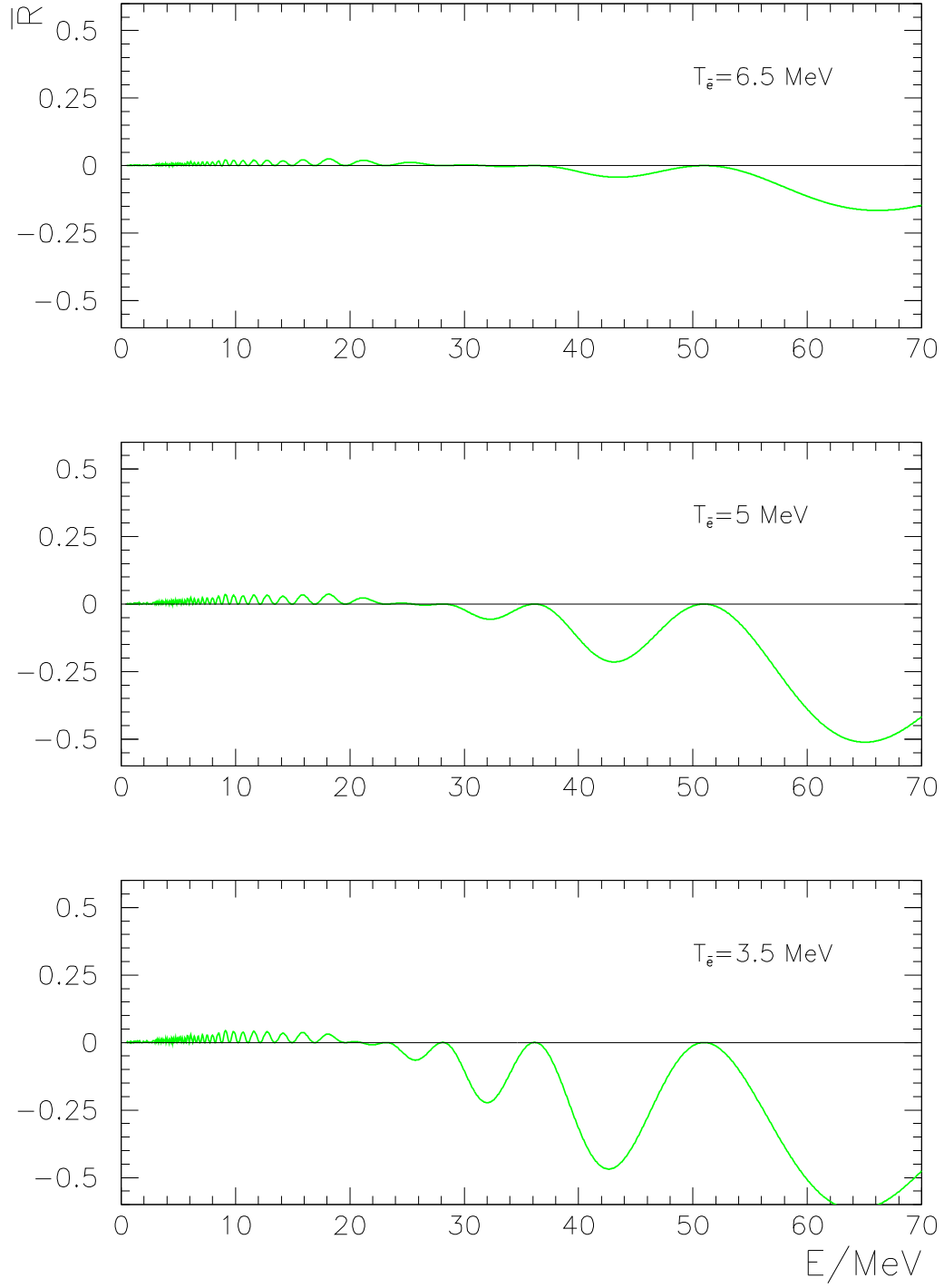


Figure 6: The same as fig. 4 for  $\theta_n = 60^\circ$  and various values of  $T_e$ .

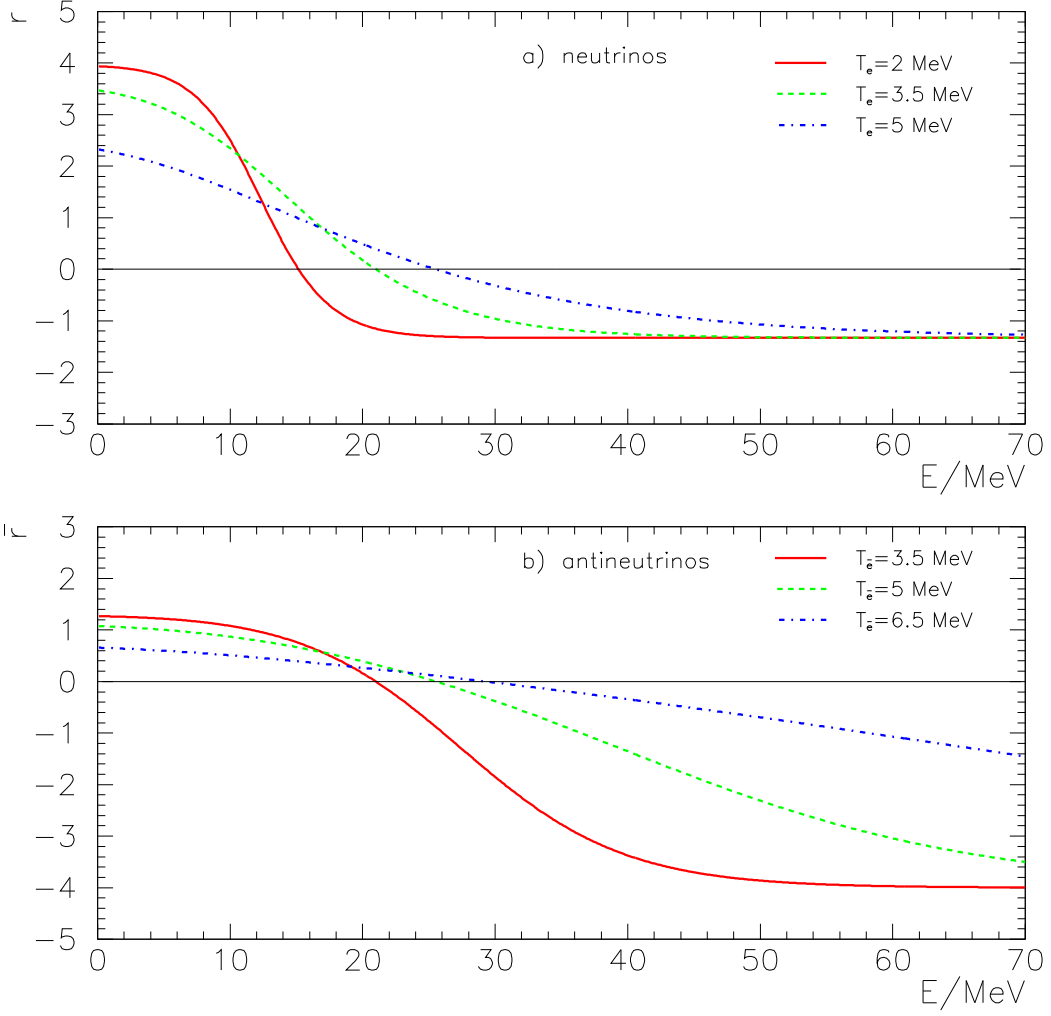


Figure 7: The flux factors  $r$  and  $\bar{r}$  for various values of the temperatures  $T_e$  and  $T_{\bar{e}}$ . We have taken  $T_x = 8 \text{ MeV}$ ,  $\Delta m_{\odot}^2 = 5 \cdot 10^{-5} \text{ eV}^2$ ,  $\sin^2 2\theta_{\odot} = 0.75$  and  $P_H = 1$ .



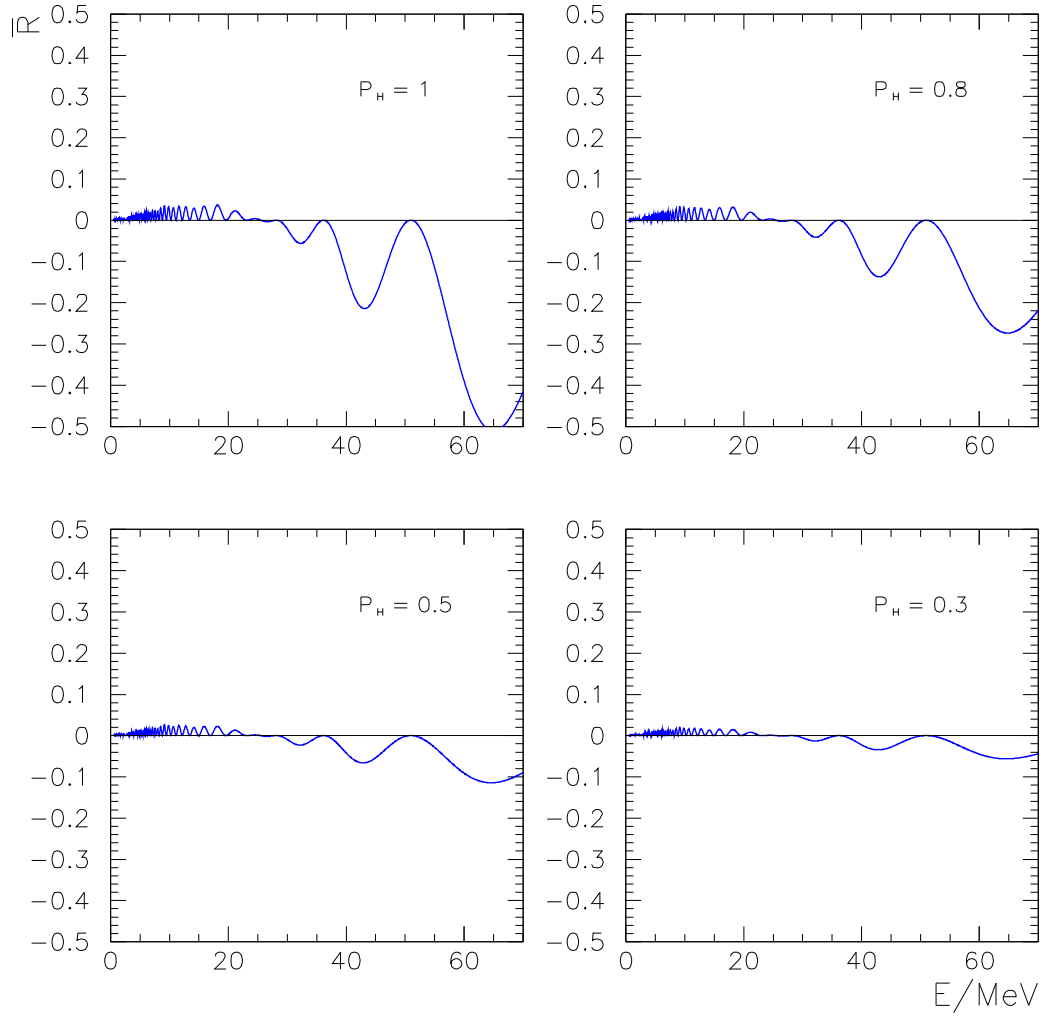


Figure 8: The same as fig. 4 for inverted mass hierarchy and various values of  $P_H$ . We have taken  $\theta_n = 60^\circ$ .

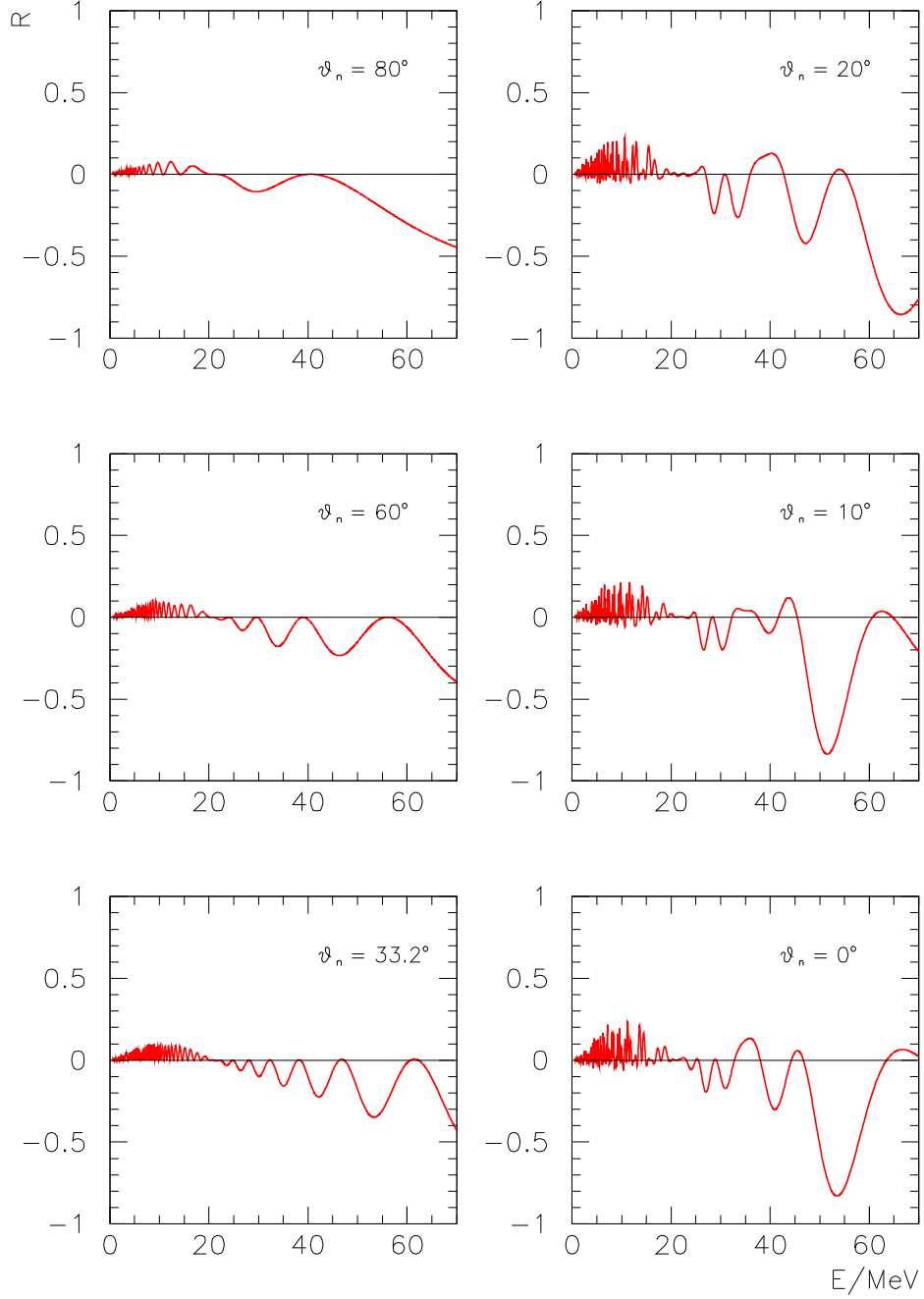


Figure 9: The relative Earth matter effect in  $\nu_e$  channel,  $R$ , as function of the neutrino energy for LMA oscillation parameters and various values of the nadir angle  $\theta_n$ . We have taken  $\Delta m_{\odot}^2 = 5 \cdot 10^{-5} \text{ eV}^2$ ,  $\sin^2 2\theta_{\odot} = 0.75$ ;  $T_e = 3.5 \text{ MeV}$ ,  $T_x = 8 \text{ MeV}$ ;  $P_H = 1$  (or inverted hierarchy).

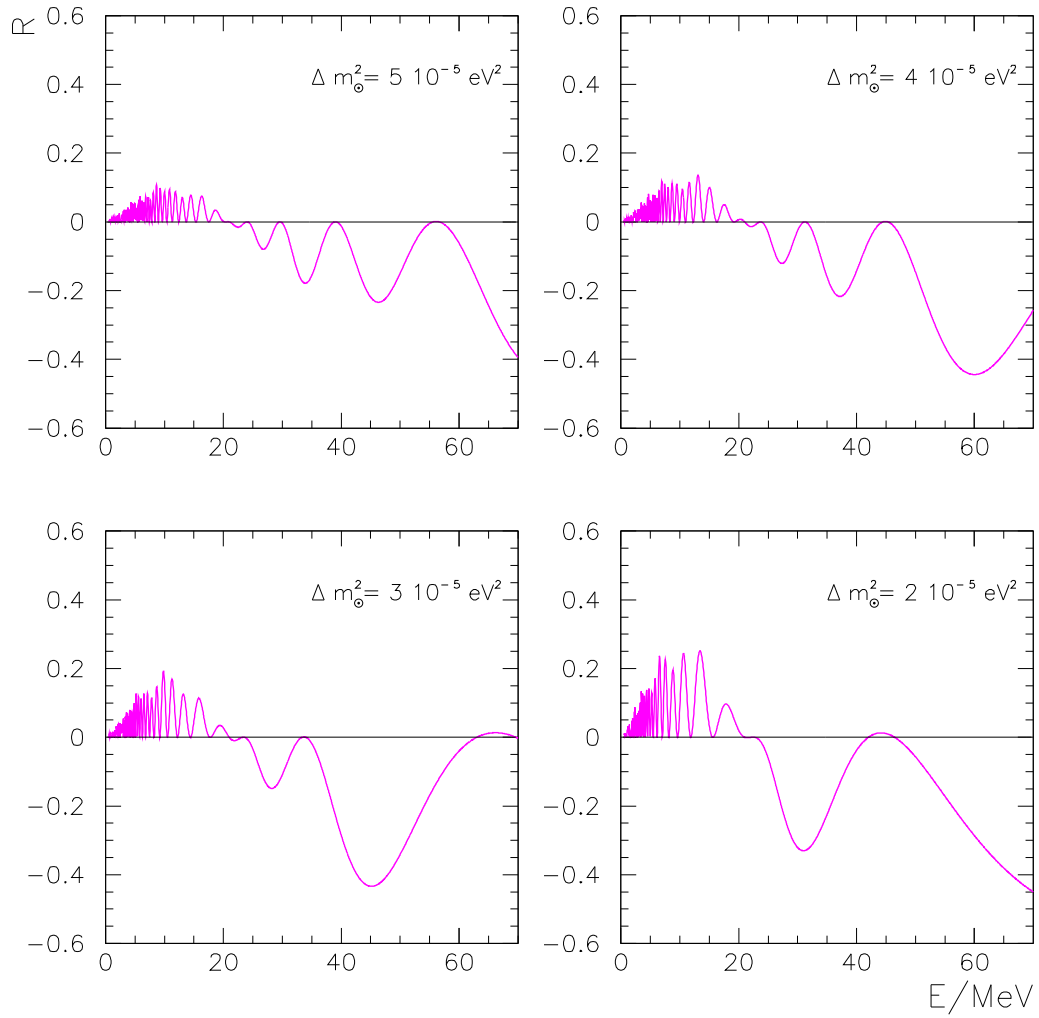


Figure 10: The same as fig. 9 for  $\theta_n = 60^\circ$  and various values of  $\Delta m_\odot^2$ .

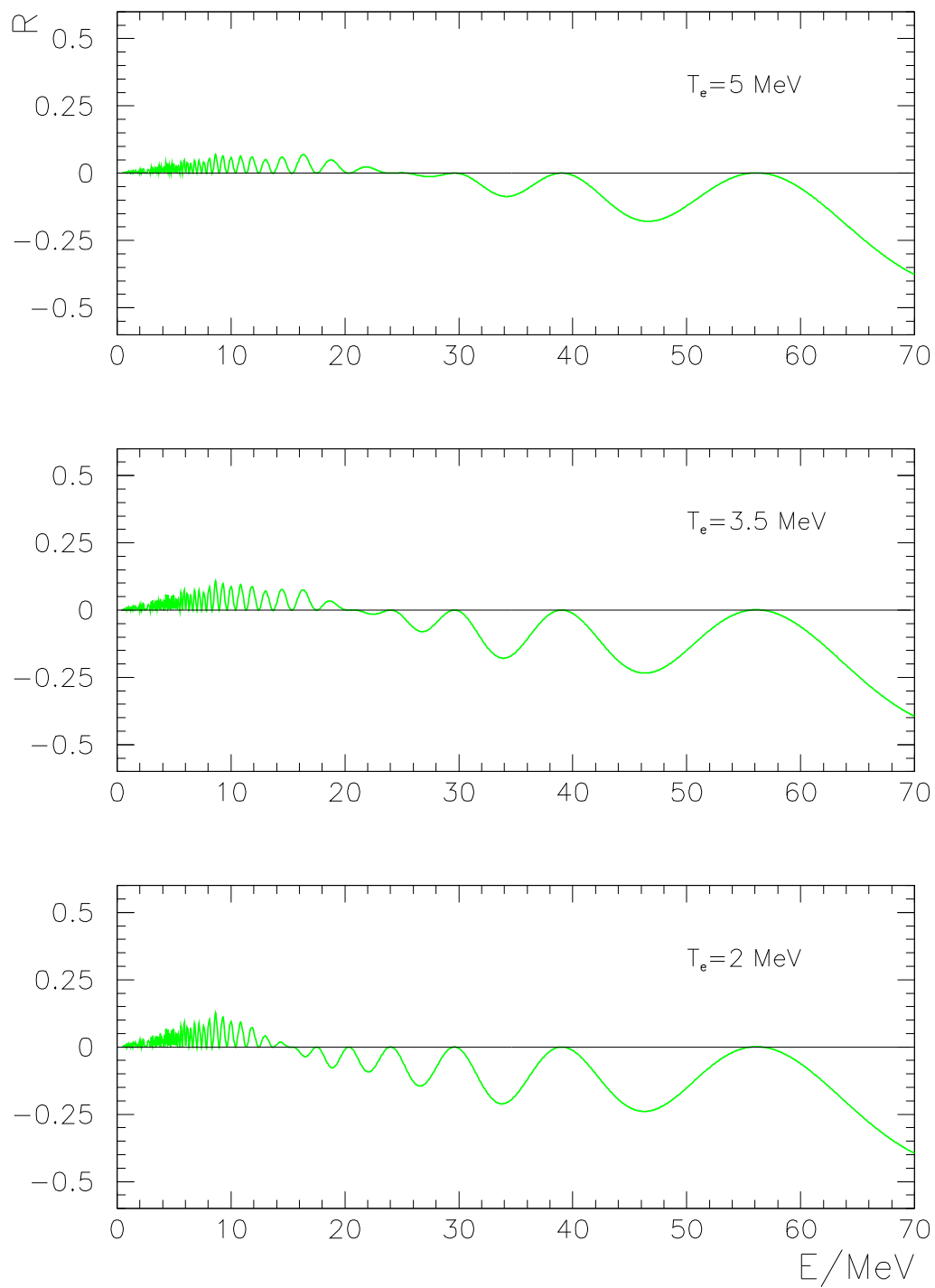


Figure 11: The same as fig. 9 for  $\theta_n = 60^\circ$  and various values of  $T_e$ .

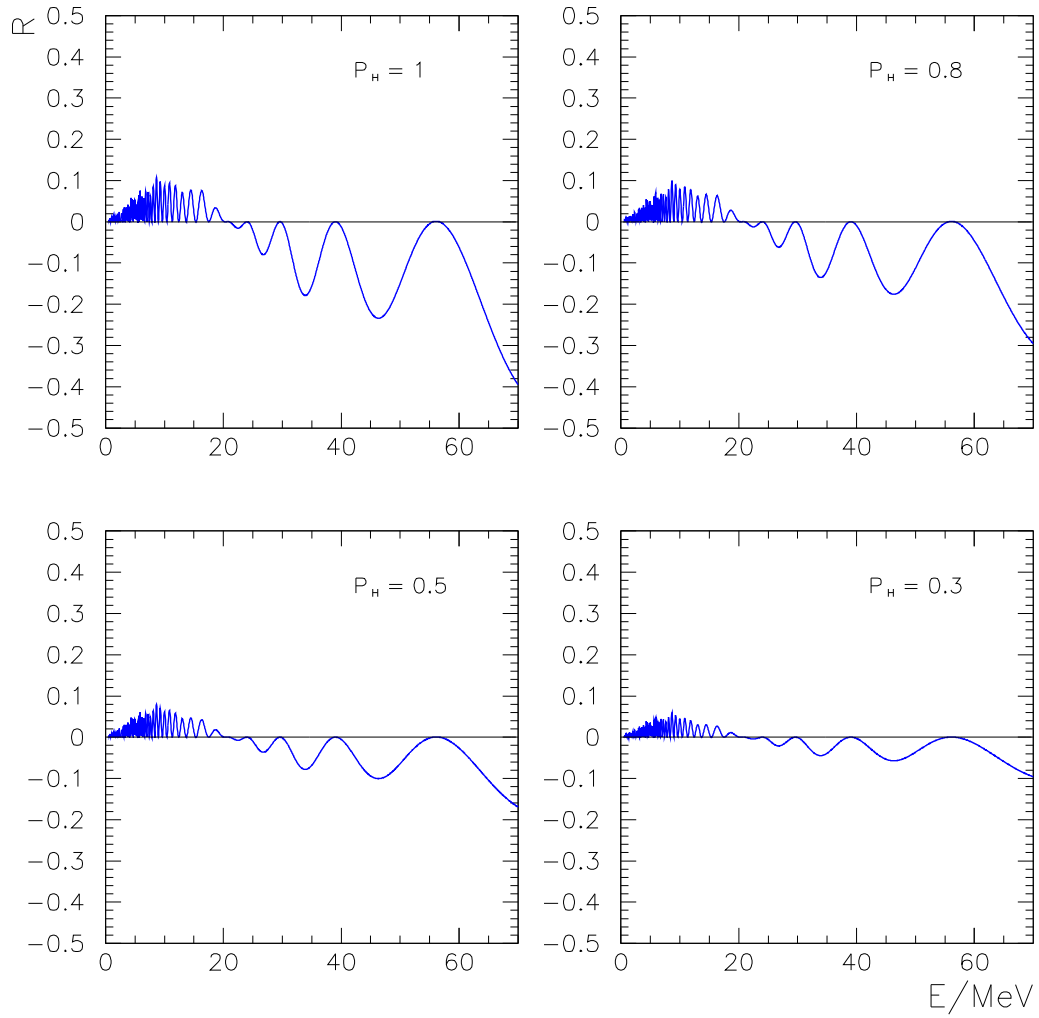


Figure 12: The same as fig. 9 for  $\theta_n = 60^\circ$  and various values of  $P_H$ .

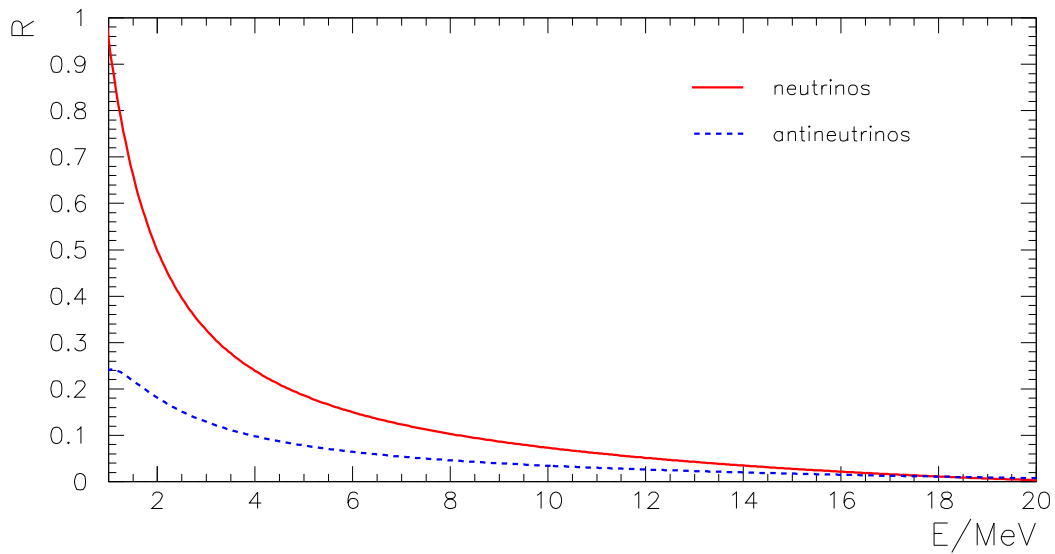


Figure 13: The relative deviations  $R$  (solid line) and  $\bar{R}$  (dashed line) as functions of the neutrino (antineutrino) energy for LOW oscillation parameters. We have taken  $\Delta m_{\odot}^2 = 10^{-7} \text{ eV}^2$ ,  $\sin^2 2\theta_{\odot} = 0.9$ ;  $T_e = 3.5 \text{ MeV}$ ,  $T_{\bar{e}} = 5 \text{ MeV}$ ,  $T_x = 8 \text{ MeV}$  and  $\theta_n = 25^\circ$ . We have also assumed  $P_H = 1$  and  $P_L = 0$ .

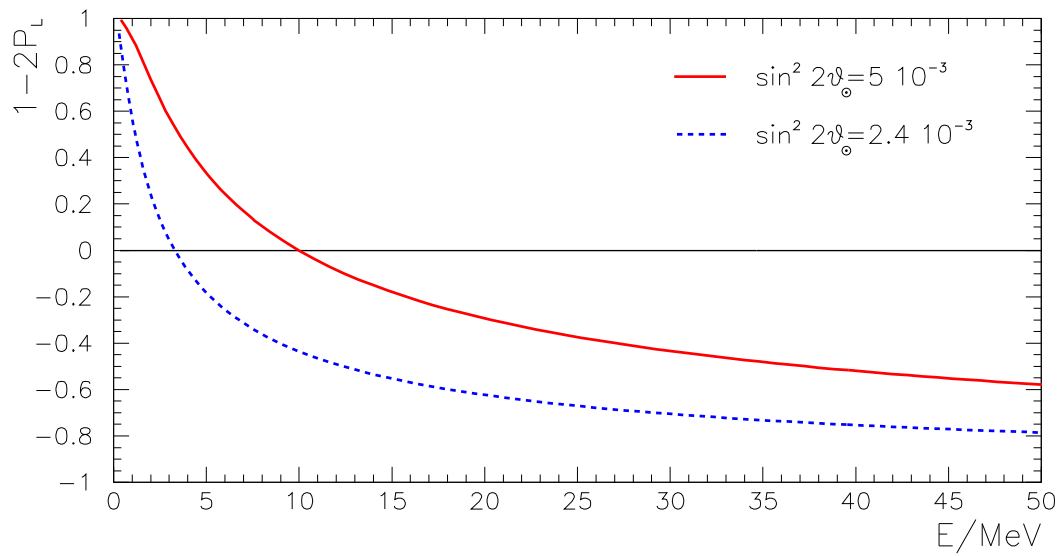


Figure 14: The quantity  $1-2P_L$  as a function of the neutrino energy for  $\Delta m_\odot^2 = 6 \cdot 10^{-6} \text{ eV}^2$  and different values of  $\sin^2 2\theta_\odot$  in the SMA region. We have taken  $C = 4$  in the profile (4).

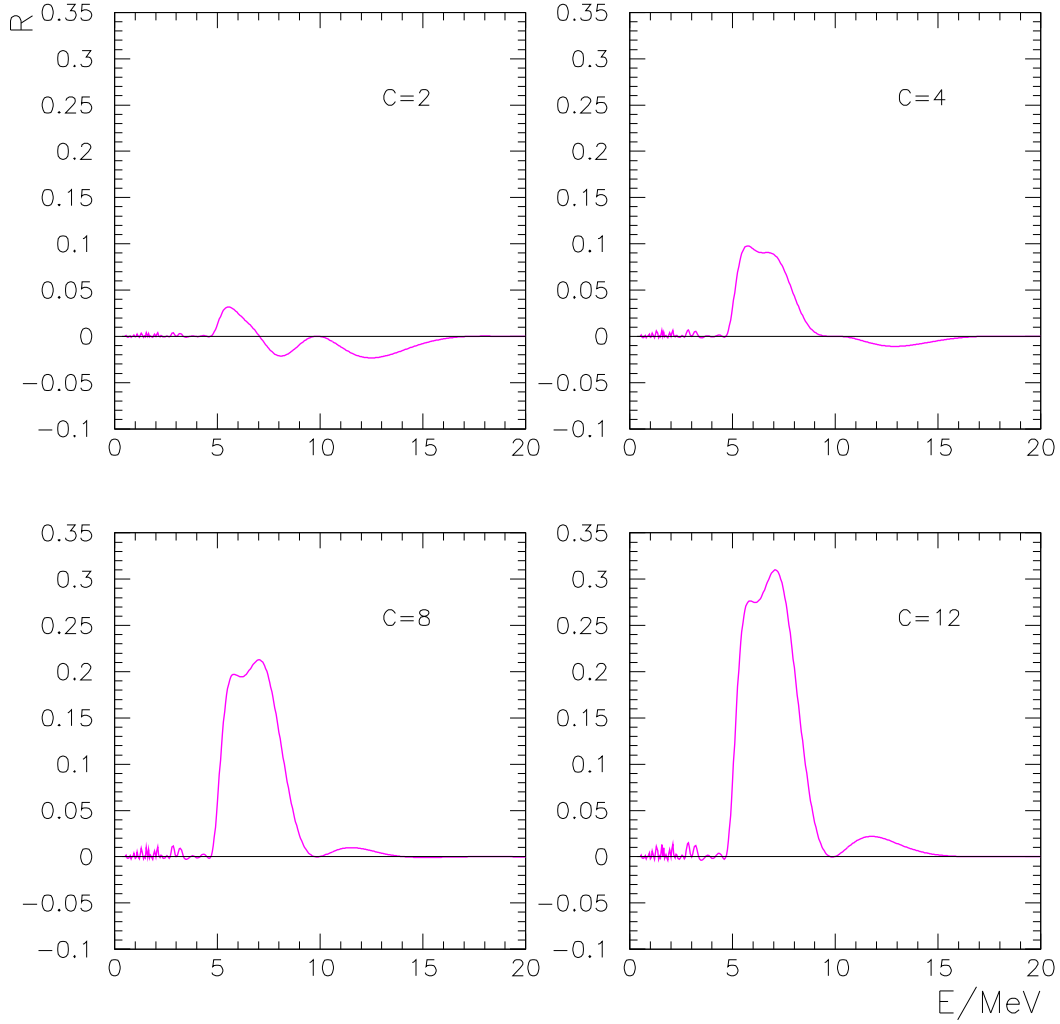


Figure 15: The relative Earth matter effect in  $\nu_e$  channel,  $R$ , as function of the neutrino energy for SMA oscillation parameters and various values of the density profile factor  $C$ . We have taken  $\Delta m_{\odot}^2 = 6 \cdot 10^{-6} \text{ eV}^2$ ,  $\sin^2 2\theta_{\odot} = 5 \cdot 10^{-3}$ ;  $T_e = 3.5 \text{ MeV}$ ,  $T_x = 8 \text{ MeV}$ ;  $P_H = 1$  (or inverted hierarchy);  $\theta_n = 0^\circ$ .



t=1 hour

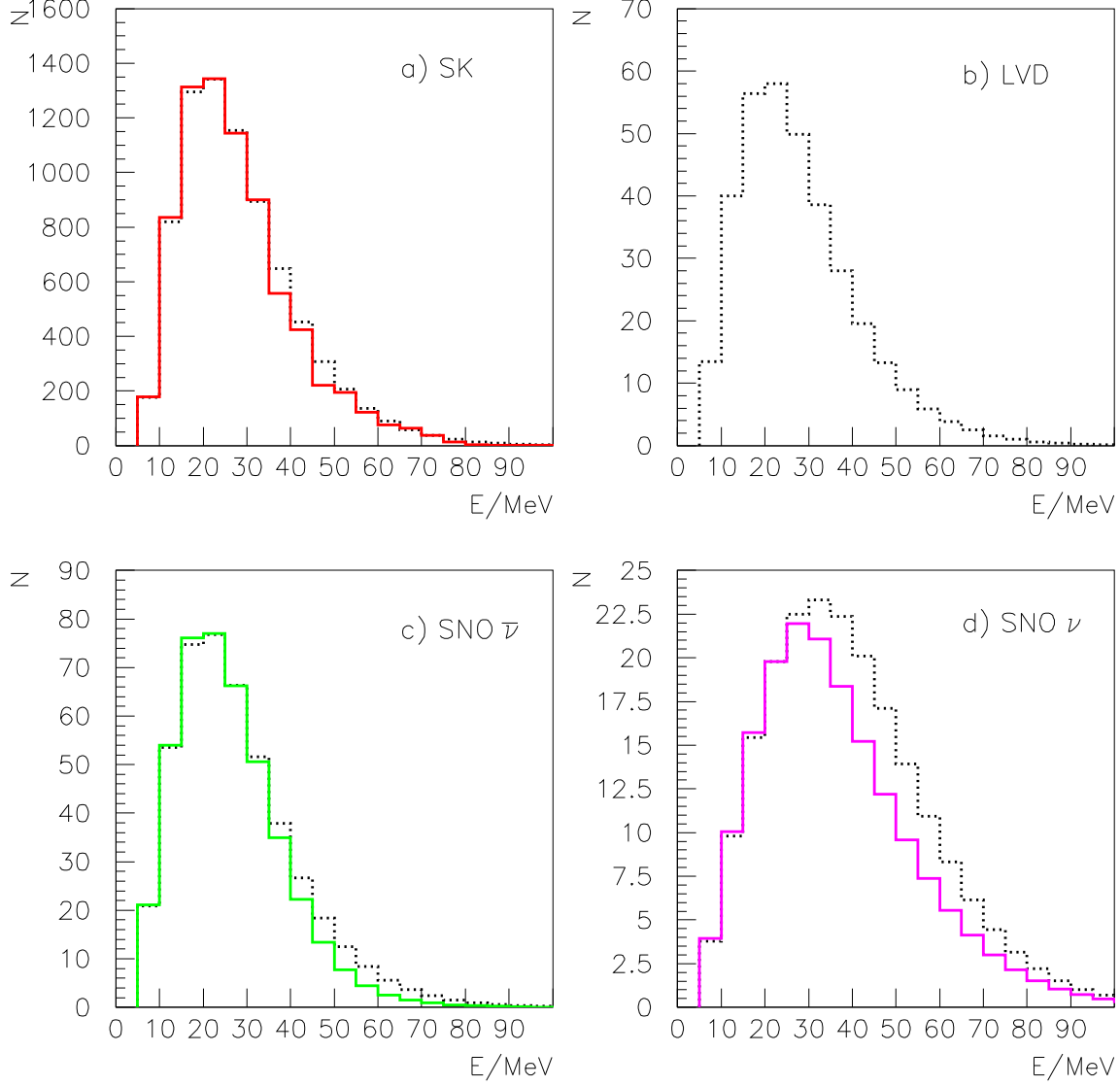


Figure 16: The energy spectra expected at SK, SNO and LVD with (solid lines) and without (dotted lines) Earth matter effect, for the same parameters as in figs. 4 and 9 and  $t = 1$  hour of fig. 1 a). A distance  $D = 10$  Kpc from the supernova and binding energy  $E_B = 3 \cdot 10^{53}$  ergs have been taken. In this specific configuration LVD is not shielded by the Earth, thus observing undistorted spectrum. The histogram c) refers to the sum of events from  $\bar{\nu}_e + p \rightarrow e^+ + n$  and  $\bar{\nu}_e + d \rightarrow e^+ + n + n$  scatterings, while the panel d) shows the events from  $\nu_e + d \rightarrow e + p + p$ . In a) and b) only the events from  $\bar{\nu}_e + p \rightarrow e^+ + n$  are shown.

t=1 hour

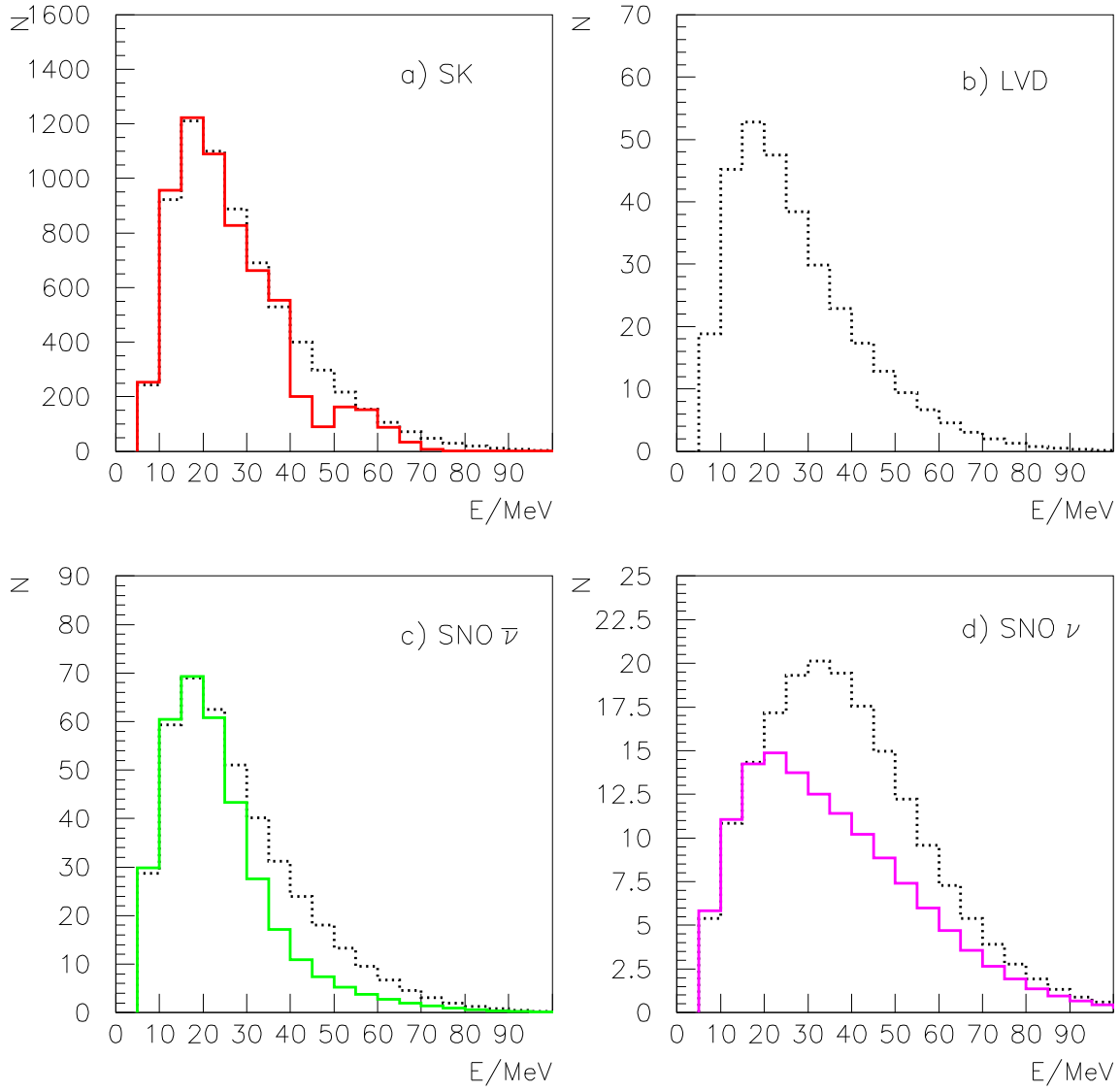


Figure 17: The same as fig. 16 for different values of some parameters:  $\Delta m_{\odot}^2 = 3 \cdot 10^{-5} \text{ eV}^2$ ,  $\sin^2 2\theta_{\odot} = 0.9$ ;  $T_e = 3 \text{ MeV}$ ,  $T_{\bar{e}} = 4 \text{ MeV}$ .

t=8 hours

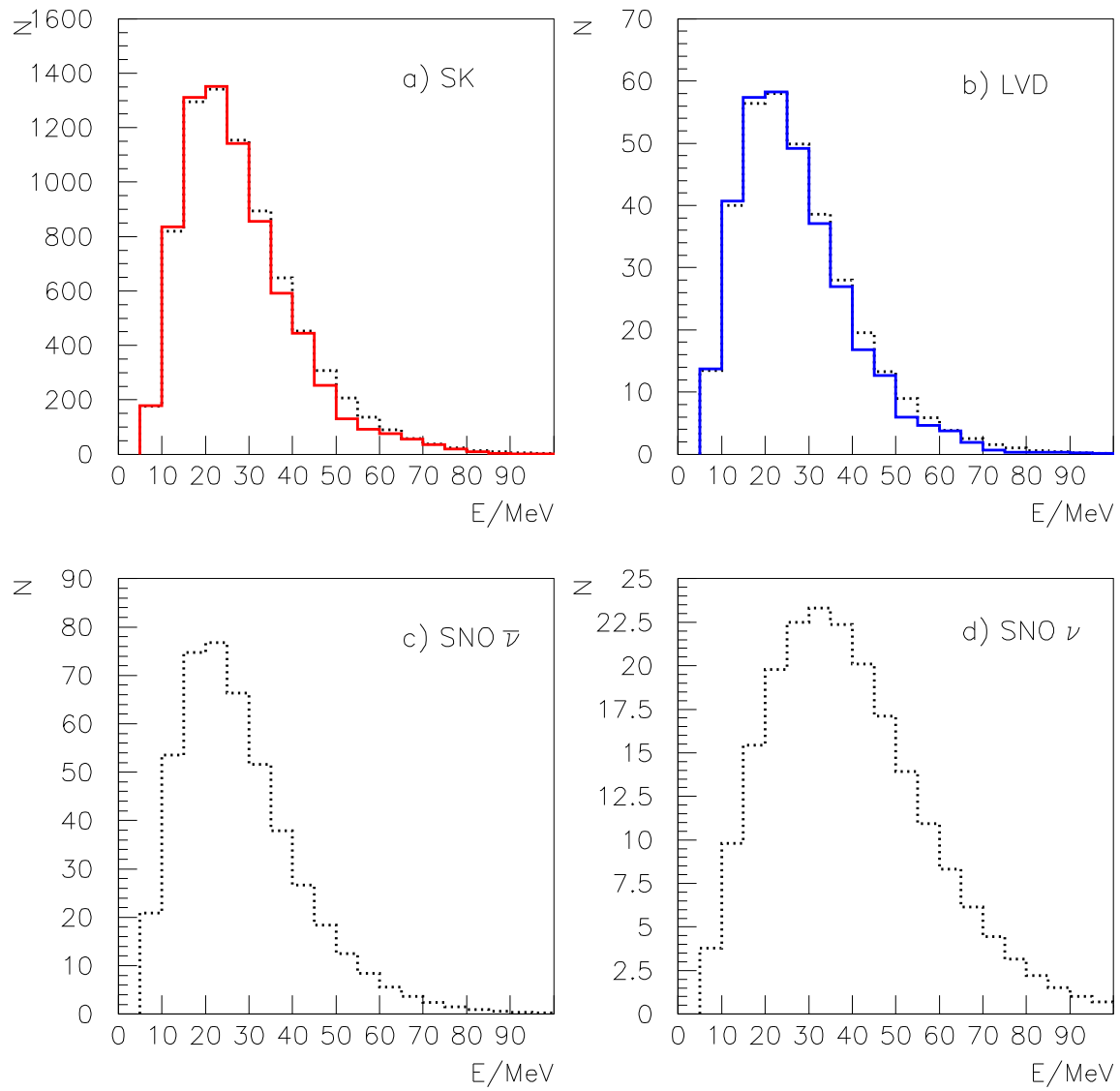


Figure 18: The same as fig. 16 for  $t = 8$  hours of fig. 1 a). For this configuration SNO is unshielded by the Earth.

t=17 hours

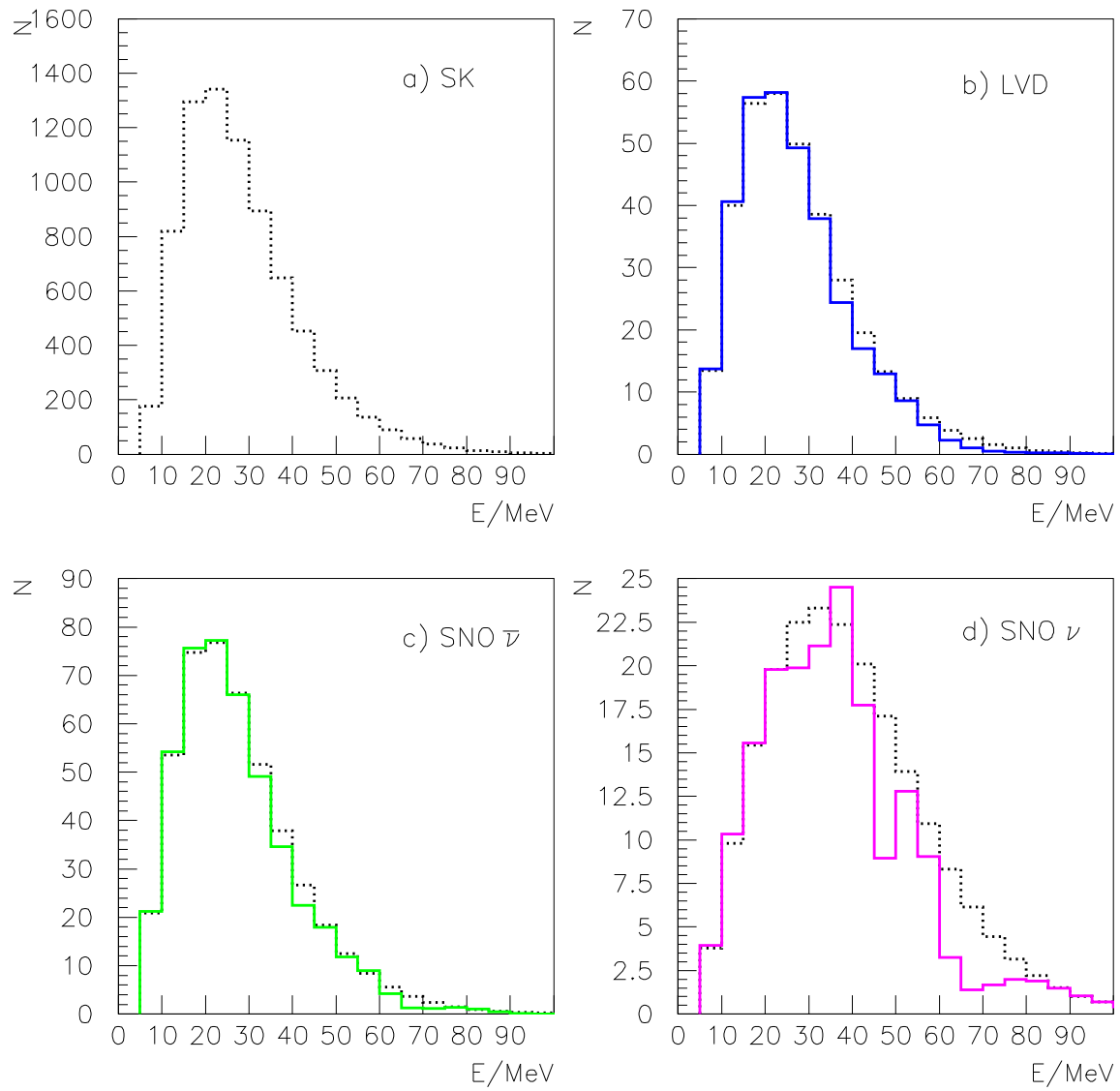


Figure 19: The same as fig. 16 for  $t = 17$  hours of fig. 1 a). For this configuration SK is unshielded by the Earth.

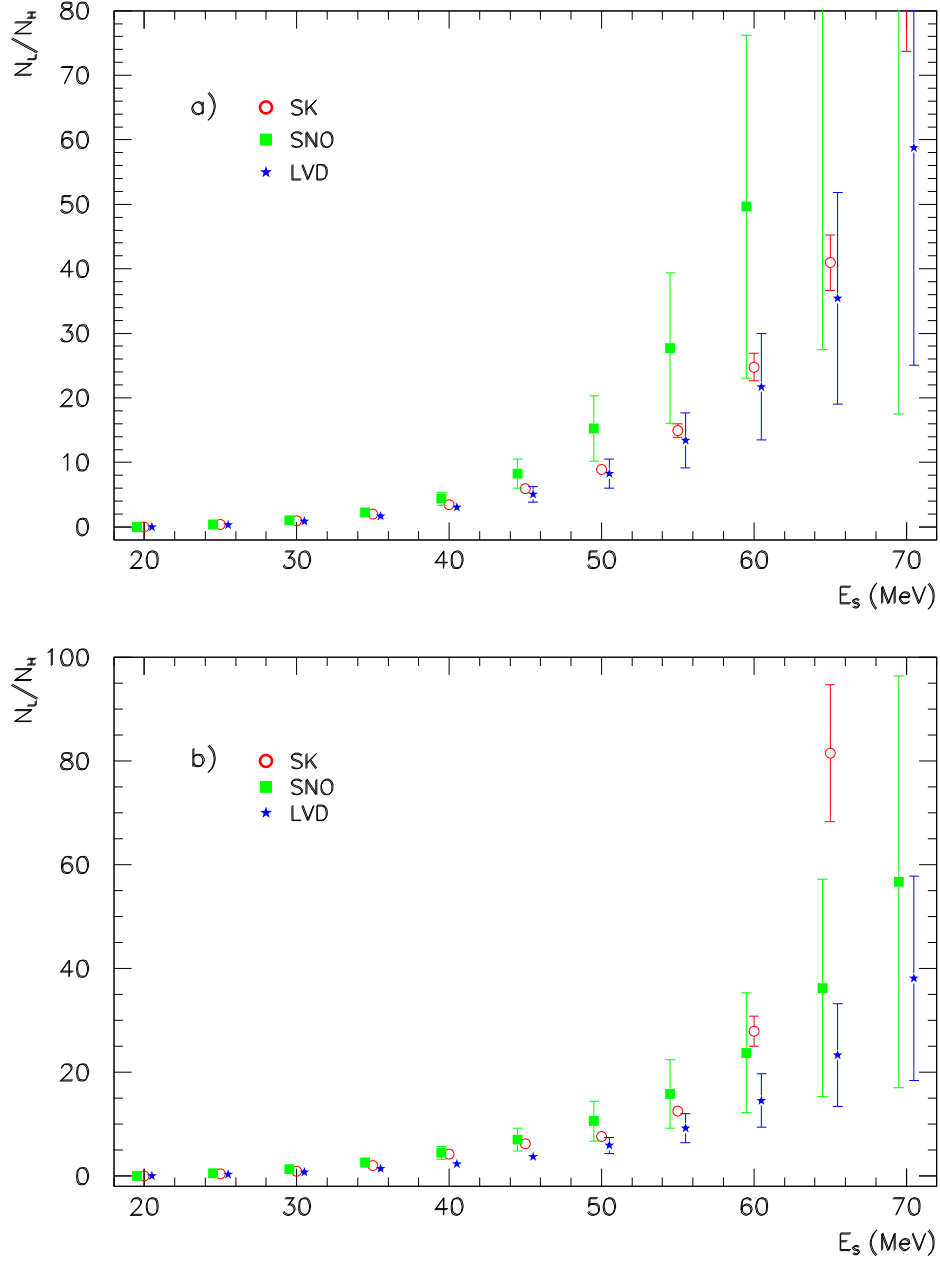


Figure 20: The ratio of the numbers of low and high-energy events from  $\bar{\nu}_e + p \rightarrow e^+ + n$  reaction at SK, SNO and LVD, as a function of the separation energy  $E_s$ . The bars represent  $1\sigma$  statistical errors. The panels a) and b) refer to the spectra shown in figs. 16 and 17 respectively. We have taken a minimum energy  $E_{th} = 20$  MeV for the calculation of the numbers of low-energy events.

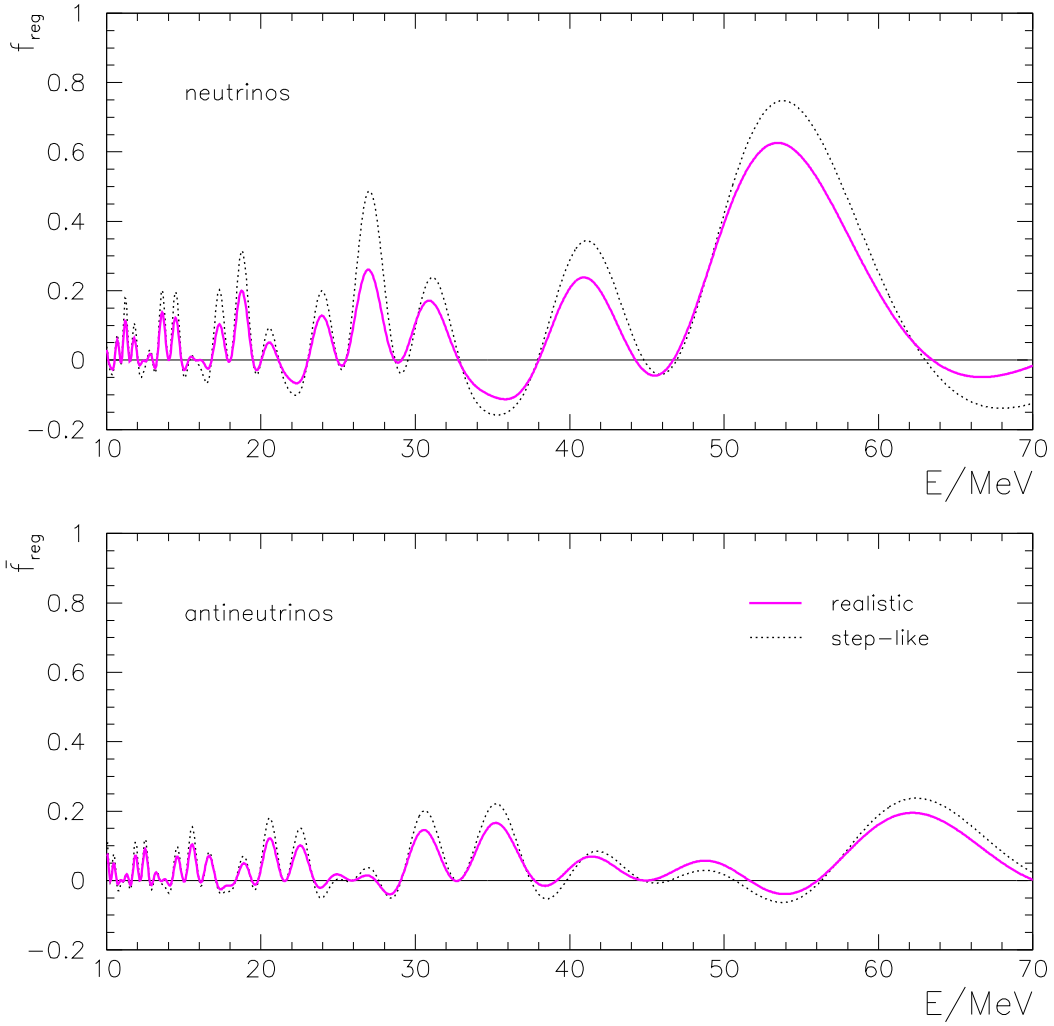


Figure 21: The regeneration factors for neutrinos,  $f_{reg}$ , and antineutrinos,  $\bar{f}_{reg}$ , calculated with step-like (two layers) and realistic profiles. We have taken  $\Delta m^2 = 5 \cdot 10^{-5} \text{ eV}^2$ ,  $\sin^2 2\theta = 0.75$ ,  $\theta_n = 0^\circ$  and the densities  $\rho_m = 4.51$  and  $\rho_c = 11.95$  for the two-layers profile.